MINISTÈRE DE L'ÉNERGIE ET DES RESSOURCES NATURELLES (MERN)

FALCON® Airborne Gravity Gradiometer and Magnetometer Survey

Baie-James, Bloc EST & OUEST, Québec, Canada

Project Number: 2100365AB (117840512-20210207-06)

Date: 2022-03-28

Logistics and Processing Report

FALCON™

Xcalibur MPH (Canada) Ltd.

2505 Meadowvale Boulevard

Mississauga, Ontario, L5N 5S2

CANADA

Tel: +1 (905) 812-0212, Fax: +1 (905) 812-1504

Xcalibur MULTIPHYSICS

Exploring the world
Safer, Clearer, Better

Table of contents

Figures

Tables

1 INTRODUCTION

Xcalibur Multiphysics conducted a high-sensitivity aeromagnetic and **FALCON®** Airborne Gravity Gradiometer (AGG) survey over the Baie-James EST (bloc A) & Baie-James OUEST (bloc B) survey area under contract with Le Ministre de l'Énergie et des Ressources Naturelles (MERN), Québec.

1.1 Survey Location

The Baie-James bloc EST and OUEST survey area is centred on longitude 77° 00' W, latitude 52º 10' N (see the location map in *Figure 1*). The production flights took place during October 2021 and February 2022 with the first production flight taking place on October 20th and the final flight taking place on February 12th. To complete the survey area coverage a total of 25 production flights were flown.

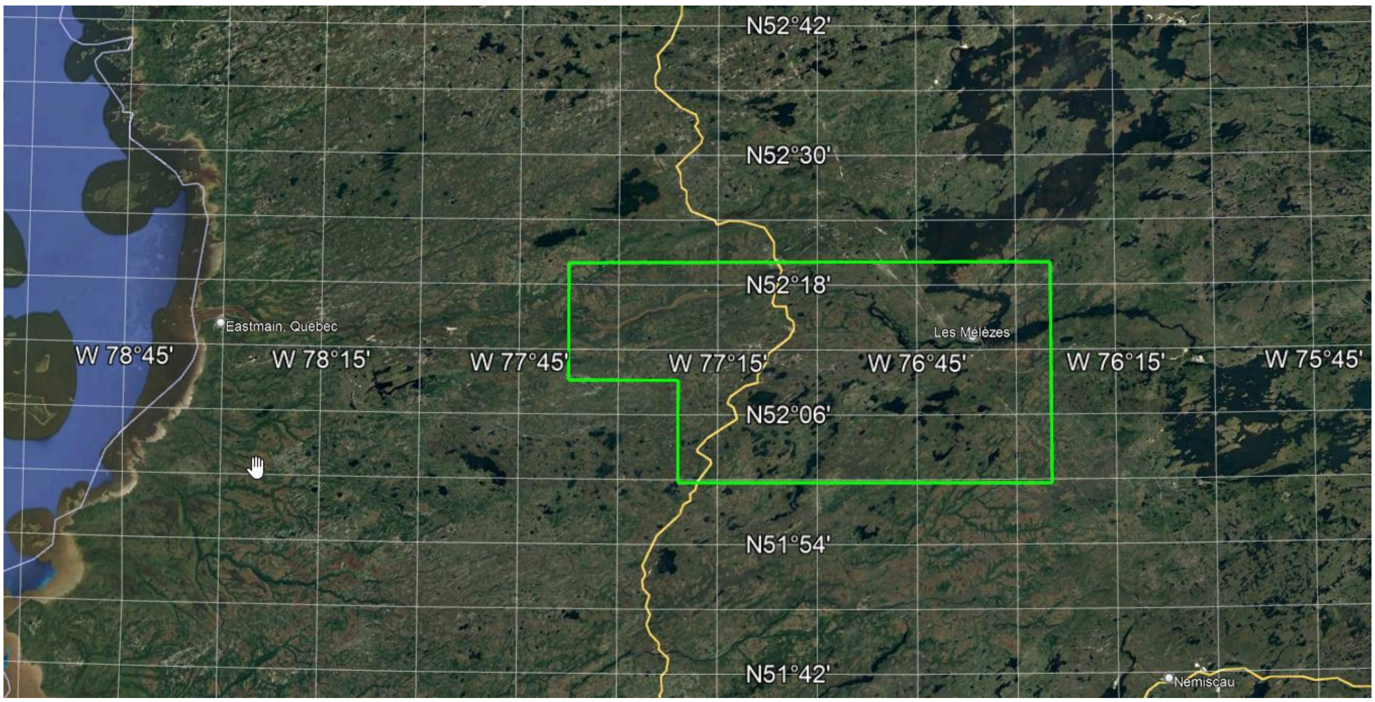

Figure 1: Baie-James bloc EST and OUEST – Survey Area Location

1.2 General Disclaimer

It is Xcalibur Multiphysics' understanding that the data and report provided to the Client are to be used for the purpose agreed between the parties. That purpose was a significant factor in determining the scope and level of the Services being offered to the Client. Should the purpose for which the data and report are used change, the data and report may no longer be valid or appropriate and any further use of, or reliance upon, the data and report in those circumstances by the Client without Xcalibur Multiphysics' review and advice shall be at the Client's own and sole risk.

The Services were performed by Xcalibur Multiphysics exclusively for the purposes of the Client. Should the data and report be made available in whole or part to any third party, and such party relies thereon, that party does so wholly at its own and sole risk and Xcalibur Multiphysics disclaims any liability to such party.

Where the Services have involved Xcalibur Multiphysics' use of any information provided by the Client or third parties, upon which Xcalibur Multiphysics was reasonably entitled to rely, then the Services are limited by the accuracy of such information.

Xcalibur Multiphysics is not liable for any inaccuracies (including any incompleteness) in the said information, save as otherwise provided in the terms of the contract between the Client and Xcalibur Multiphysics.

2 SUMMARY OF SURVEY PARAMETERS

2.1 Survey Area Specifications

Total Kilometres (km)	12,521
Clearance Method	Drape
Minimum Drape Height (m	80
Traverse Line Direction (deg.)	2°/182°
Traverse Line Spacing (m)	250
Tie Line Direction (deg.)	92°/272°
Tie Line Spacing (m)	2500

Table 1: Baie-James bloc EST and OUEST – Specifications

The survey block is defined by the coordinates in *Table 2*, in UTM Zone 18N projection, referenced to the WGS84 datum.

Baie-James EST (bloc A)			Baie-James OUEST (bloc B)		
Corner Number	**Easting**	**Northing**	**Corner Number**	**Easting**	**Northing**
1	403645	5799240	1	364126	5800060
2	393849	5799441	2	354332	5800339
3	382855	5799690	3	342339	5800708
4	372460	5799948	4	332219	5801043
5	367111	5800092	5	332219	5831051
6	367113	5839924	6	332413	5831070
7	367291	5840003	7	330941	5845985
8	361228	5853757	8	330742	5845965
9	361045	5853676	9	332209	5831100
10	367103	5839933	10	332210	5801043
11	367101	5800092	11	331346	5801072
12	363665	5800184	12	321152	5801432
13	363663	5800116	13	321148	5801304
14	362626	5762536	14	320423	5781318
15	362658	5762372	15	320610	5781298
16	373052	5762096	16	328605	5781015
17	381848	5761880	17	339198	5780661
18	393442	5761619	18	339369	5780627
19	403038	5761424	19	338806	5763237
20	403061	5761604	20	338849	5763084
21	403792	5799186	21	346245	5762850
			22	352641	5762657
			23	363035	5762361
			24	363106	5762493
			25	364134	5799872

Table 2: Baie-James bloc EST and OUEST – Survey Boundary Coordinates

2.2 Data Recording

The following parameters were recorded during the course of the survey:

- **FALCON® AGG data:** recorded at different intervals.
- **Airborne total magnetic field:** recorded with a 0.1 s sampling rate.
- **Terrain clearance:** provided by the radar altimeter at intervals of 0.1 s.
- **Airborne GPS positional data** (latitude, longitude, height, time and raw range from each satellite being tracked): recorded at intervals of 1 s.
- **Time markers:** in digital data.
- **Ground total magnetic field:** recorded with a 1 s sampling rate.
- **Ground based GPS positional data** (latitude, longitude, height, time and raw range from each satellite being tracked): recorded at intervals of 1 s.

- **Ground surface below aircraft:** mapped by the laser scanner system (when within range of the instrument and in the absence of thick vegetation), scanning at multiple frequencies (36HZ and 50Hz).

2.3 Project Safety Plan, HSE Summary

A Job Safety Plan and Job Safety Analysis was prepared and implemented in accordance with the Xcalibur Multiphysics Occupational Safety and Health Management System.

3 FIELD OPERATIONS

3.1 Operations

The survey was based out of James Bay Region, Québec. The survey aircraft was operated from La Grande Rivière Airport using aviation fuel available on site. A temporary office was set up in Radisson where all survey operations were run, and the post-flight data verification was performed.

3.2 Base Stations

A dual frequency GPS base station was set up at La Grande Rivière Airport in order to correct the raw GPS data collected in the aircraft. A secondary GPS base station was available during the survey.

3.2.1 GPS Base Station

Primary: from October 21 until November 03, 2021

Location:	La Grande Rivière Airport
Date:	October 20st, 2021
Latitude:	53º 37' 36.18469" N
Longitude:	-77º 42' 06.96071" W
Height:	147.352m ellipsoidal

Primary: from February 05, 2022 until the end of the survey

Location:	La Grande Rivière Airport
Date:	October 20st, 2021
Latitude:	53º 37' 35.82622" N
Longitude:	-77º 42' 05.96302" W
Height:	147.613m ellipsoidal

3.2.2 Magnetometer Base Station (CF1)

Location:	La Grande Rivière Airport
Date:	October 20st, 2021
Used for flights:	101 to 306
Base value:	56234.3 nT

3.3 Field Personnel

The following technical personnel participated in field operations:

Crew Leader:	David Patzer; Lucas Charbonneau
Pilots:	Darcy Wiens; Stephen Parks; Jarrett Krasnikoff; Neal Titanich; Tyler Sweeny; Cameron Sutcliffe
AME:	Adam Werner and Renko Canstapel
Technicians:	Johan van Rooyen
Project Manager:	Brett Robinson
QC and Processing:	Jemal Mohammed-Nour, Mohamed Abubeker, Chris van Galder

Table 3: Baie-James bloc EST and OUEST – Field Personnel

4 QUALITY CONTROL RESULTS

4.1 Survey acquisition issues

During the course of the survey, there were no data quality issues with:

- AGG instrumentation
- Magnetic and GPS base stations
- Airborne magnetometer system
- Data acquisition systems
- Laser scanner

4.2 Flight Path Map

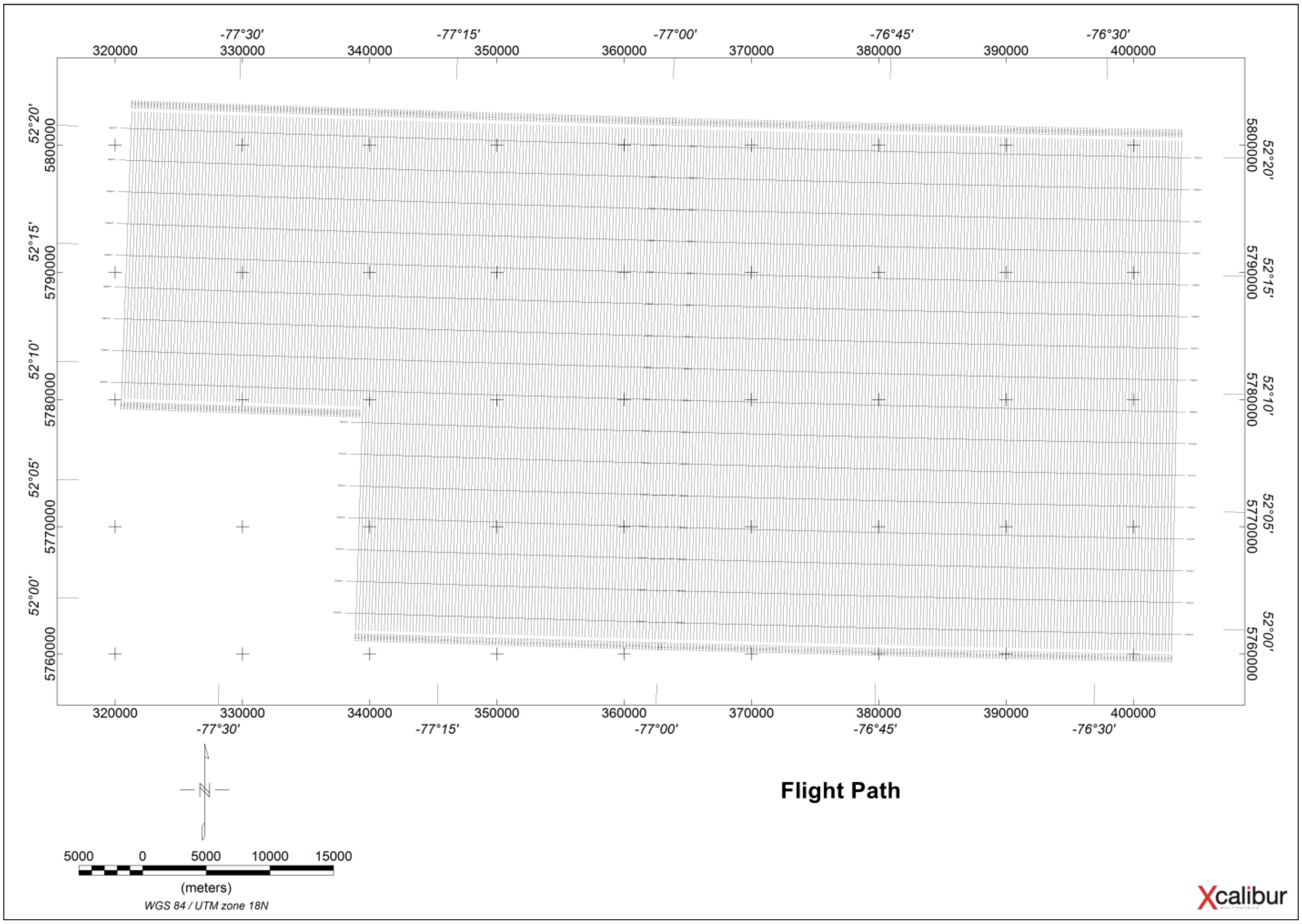

Figure 2: Baie-James bloc EST and OUEST – Flight Path map

4.3 Turbulence

The mean turbulence recorded in the Baie-James bloc EST and OUEST survey area was 42.7 milli g (where g = 9.80665 m/sec/sec). The turbulence pattern across the survey area is shown in *Figure 3*.

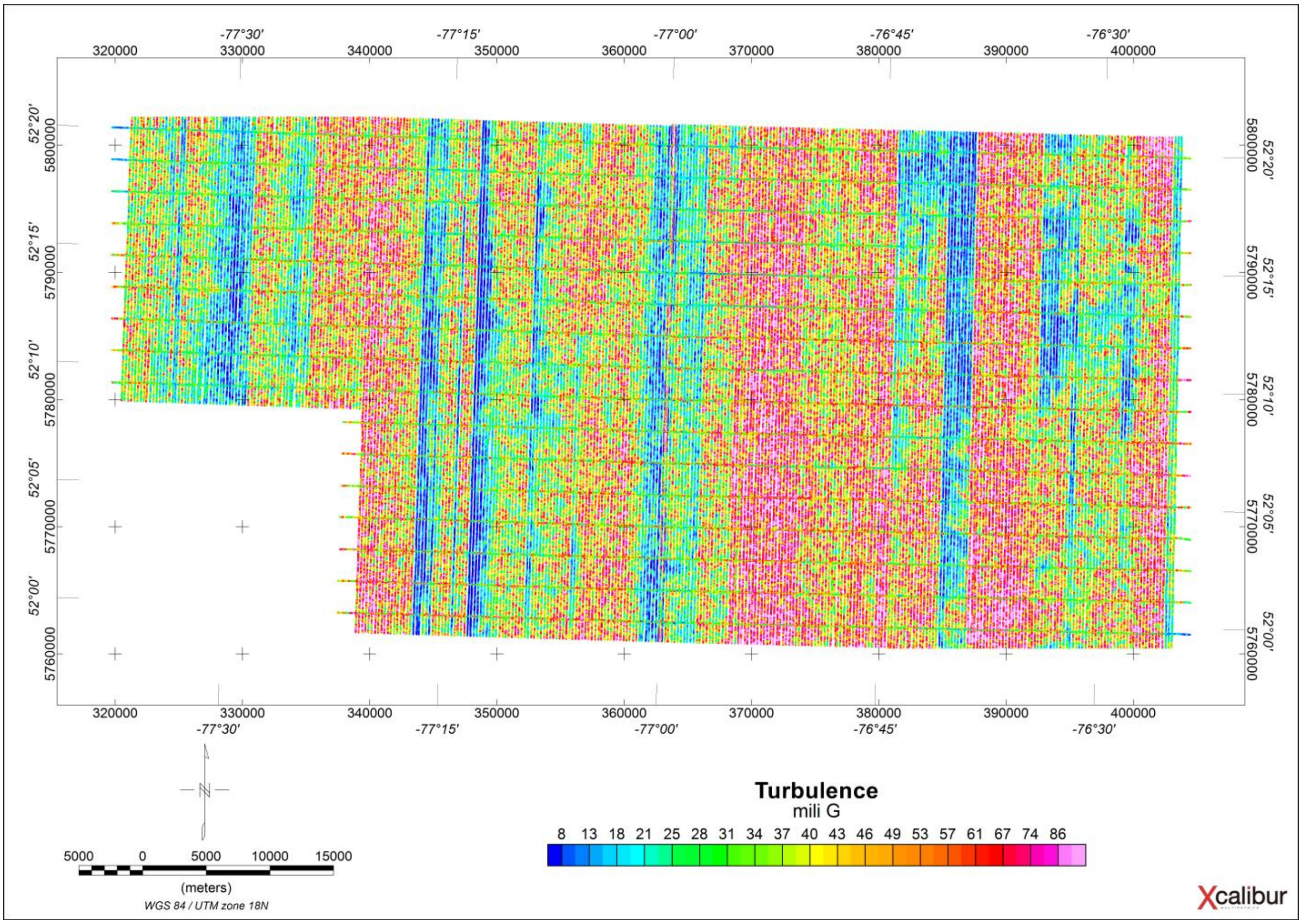

Figure 3: Baie-James bloc EST and OUEST 3 – Turbulence (milli g where g = 9.80665 m/sec/sec)

4.4 AGG System Noise

The system noise is defined to be the standard deviation of half the difference between the A & B complements, for each of the NE and UV curvature components. Both a digital AGG (Kepler) and an anolog AGG (Galileo) system were utilized on the survey installed in a Cessna Grand Caravan and a Basler aircraft respectively. The digital system inherently has a lower noise characteristic then the analog system as is evident in Figure 4 and Figure 5. The Basler aircraft with the analog system flew the area to the East of centre along with a series of lines further to the East in the block. The results for this survey were very good with overall values of 2.0 E and 1.9 E for NE and UV respectively.

Figure 4 and *Figure 5* provide a representation of the variation in this standard deviation for each component. This is achieved by gridding a rolling measurement of standard deviation along each line using a window length of 100 data points.

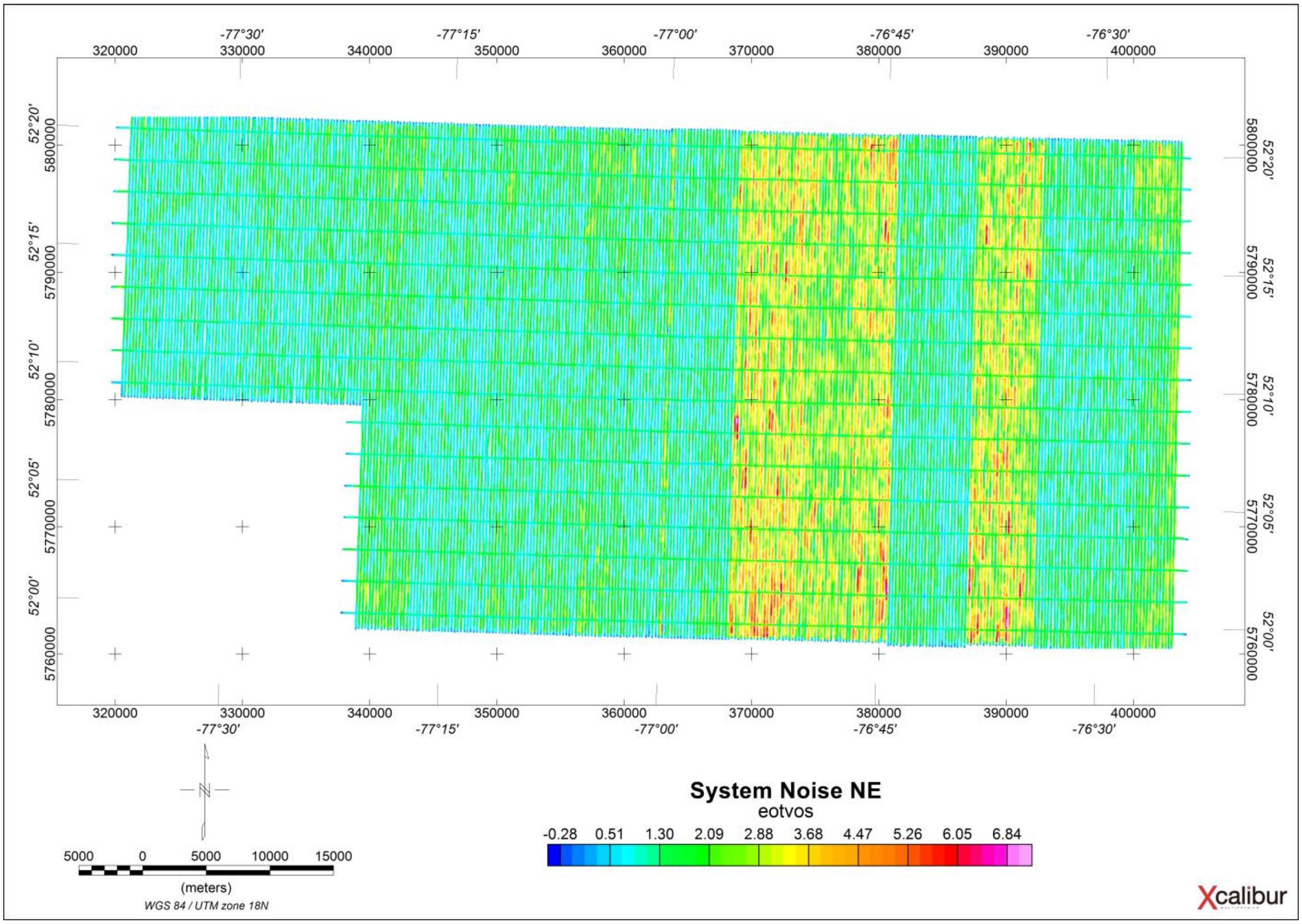

Figure 4: Baie-James bloc EST and OUEST – System Noise NE (eotvos). Areas of higher system noise were covered using the analog AGG system (Galileo).

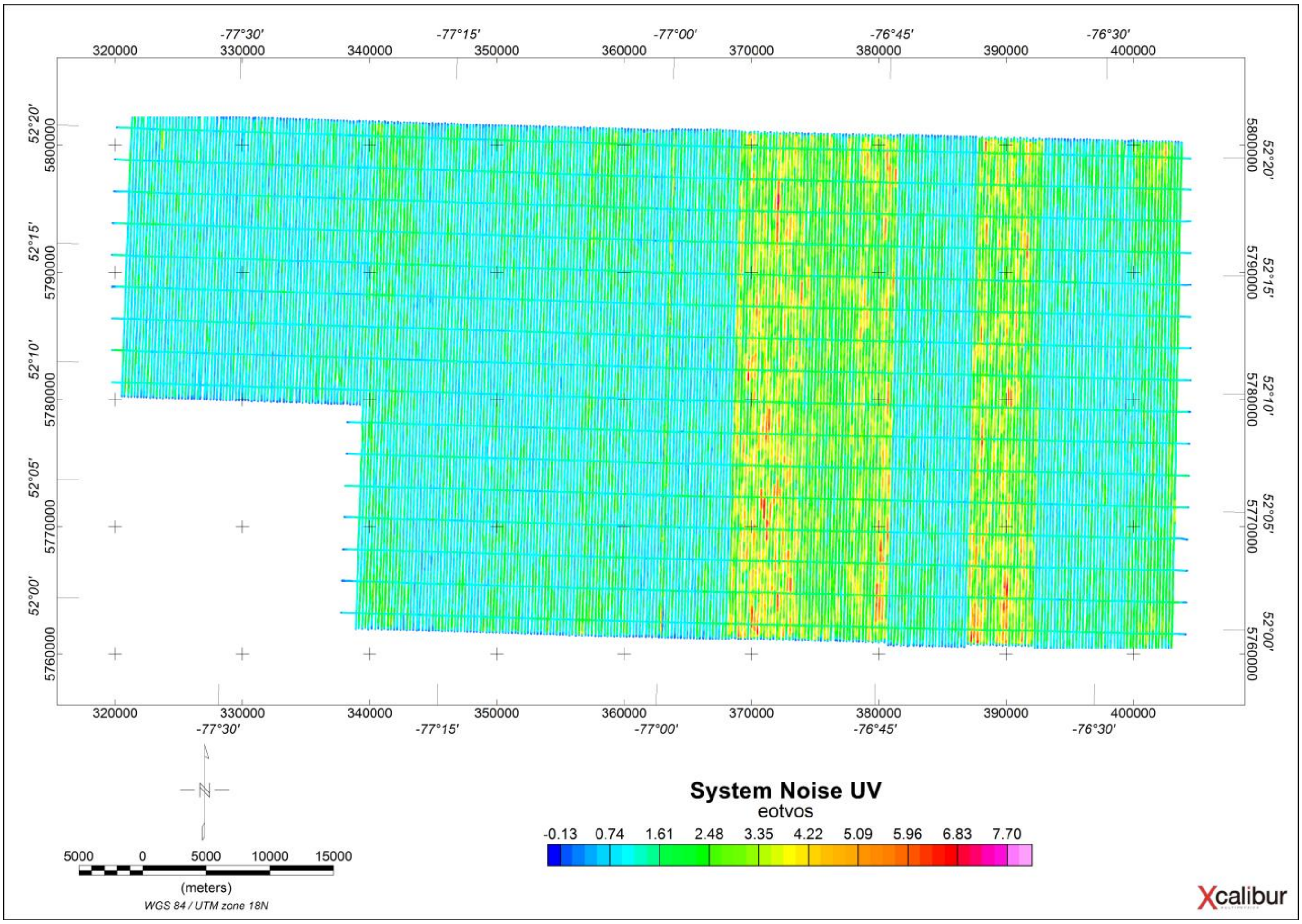

Figure 5: Baie-James bloc EST and OUEST – System Noise UV (eotvos). Areas of higher system noise were covered using the analog AGG system (Galileo).

4.5 Digital Terrain Model

Laser scanner range data were combined with GPS position and height data (adjusted from height above the WGS84 ellipsoid to height above the geoid by applying the Earth Gravitational Model 1996 (EGM96)). The output of this process is a "swath" of terrain elevations extending either side of the aircraft flight path. Width and sample density of this swath varies with aircraft height. Typical values are 180 to 250 metres and 5 to 15 metres respectively.

Because terrain correction of AGG data requires knowledge of the terrain at distances up to at least 40 km from the data location, laser scanner data collected only along the survey line path must be supplemented by data from another source.

For this purpose, Shuttle Radar Topography Mission (SRTM) v3 (one arc second resolution) data are used.

Laser scanner data quality was good with scan density generally above 90%. Laser scanner data were gridded at 25 m with a 1 cell maximum extension beyond data limits. To fill gaps between lines and extend data coverage beyond the survey area, SRTM grid data were excised to an area 40 km beyond the planned survey area. The excised data were adjusted to the level of the laser scanner data using a grid difference adjustment method. The two grids were then combined into a single grid such that unmodified laser scanner data were used where defined and adjusted SRTM data were used to fill the gaps and extend the area.

Figure 6 shows the final Digital Terrain Model for the survey area.

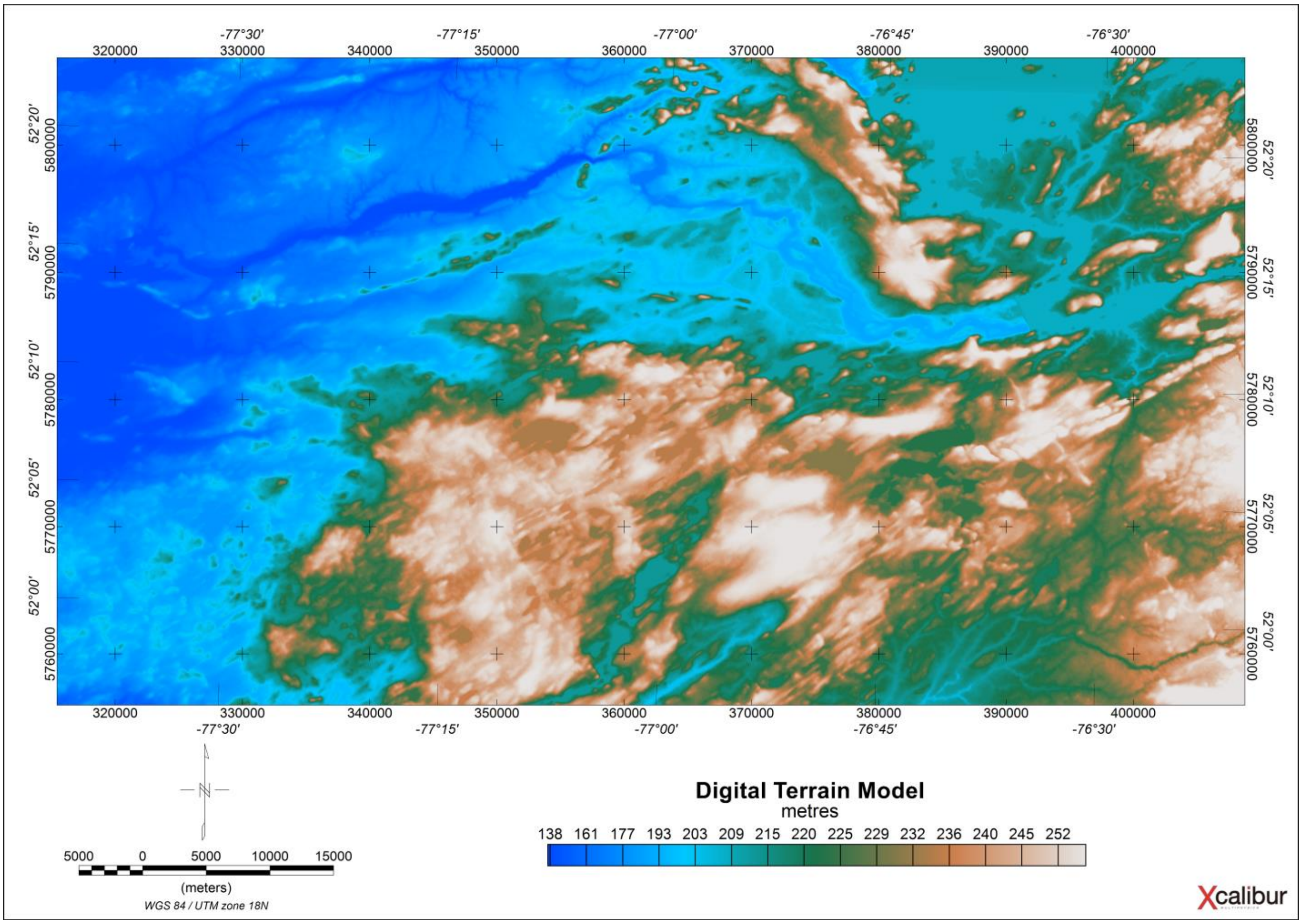

Figure 6: Baie-James bloc EST and OUEST – Final Digital Terrain Model (metres, referenced to the EGM96 geoid)

4.6 Terrain Clearance

Terrain clearance for the Baie-James bloc EST and OUEST survey averaged slightly above the nominal clearance of 80 m having a mean value of 99.0 m across the survey area. The terrain clearance, as derived from laser scanner data, is shown in *Figure 7*.

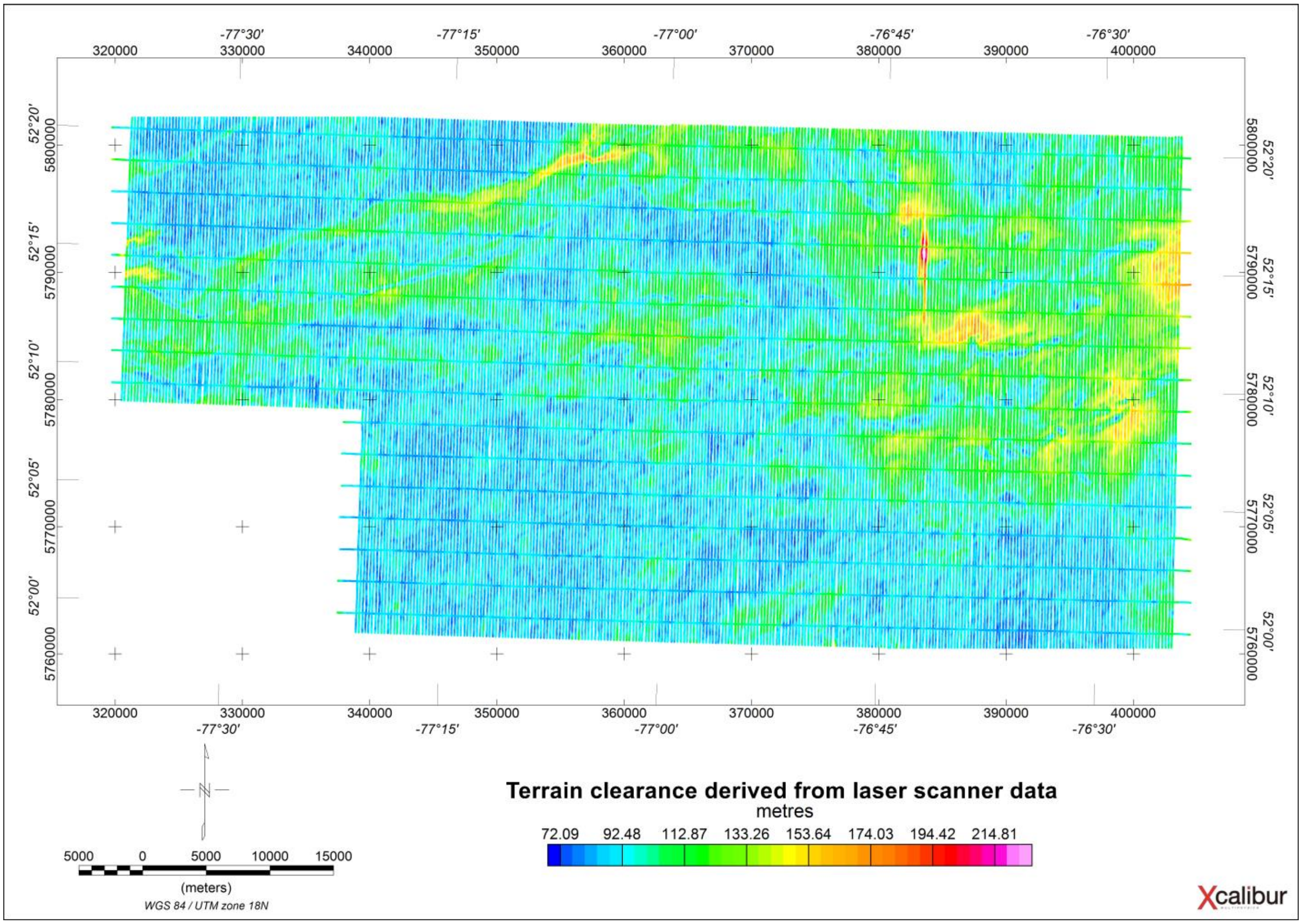

Figure 7: Baie-James bloc EST and OUEST – [Terrain clearance derived from laser scanner data (metres)]

5 FALCON® AIRBORNE GRAVITY GRADIENT (AGG) RESULTS

5.1 Processing Summary

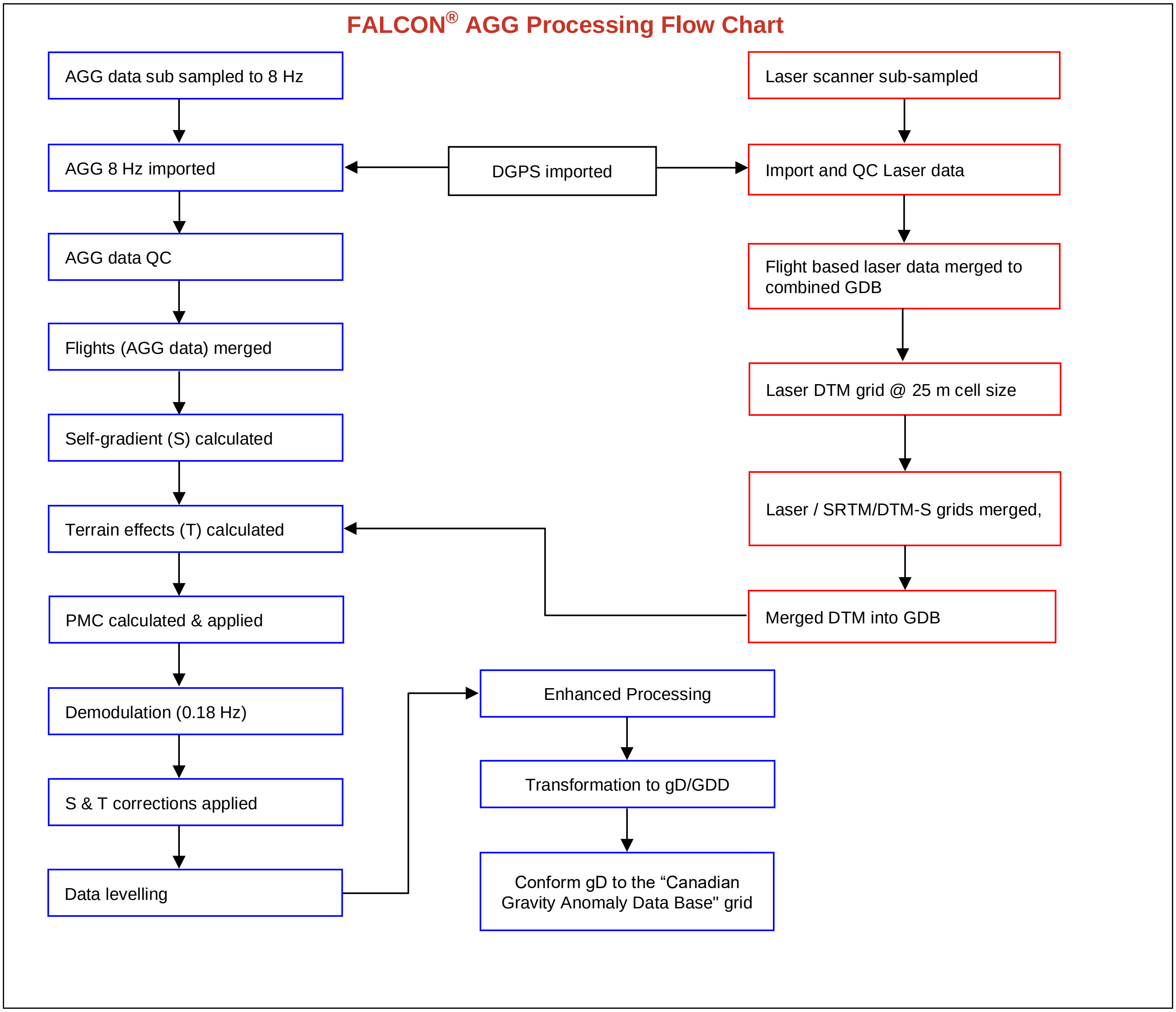

Figure 8: FALCON® AGG Data Processing

5.2 FALCON® Airborne Gravity Gradiometer Data

Figure 8 summarises the steps involved in processing the AGG data obtained from the survey.

The **FALCON®** Airborne Gravity Gradiometer data were digitally recorded by the ADAS on removable hard drives. The raw data were then copied to the field processing laptop, backed up twice onto hard disk media and transferred by Secure File Transfer to the Xcalibur Multiphysics Jandakot data processing centre.

Preliminary processing and QC of the **FALCON®** AGG data were completed on-site and at the Jandakot data processing centre using Xcalibur Multiphysics' AGG QC software. Further QC and final **FALCON®** AGG data processing were performed at the Jandakot data processing centre.

5.3 Laser Scanner Data

Laser scanner returns were recorded at a rate of 36 scans per second with each scan returning 276 data points. Each return was converted to ground surface elevation by combining scanner range and angle data with aircraft position and attitude data. Computed elevations were then sub sampled by first dividing each scan into ten segments and combining five adjacent scans per segment, then using a special algorithm to select the optimum return within each data "bin" thus formed. Sub-sampled laser scanner data were edited to remove spikes prior to gridding.

5.4 Positional Data

Differential GPS processing was applied to compute accurate aircraft positions once per second. Waypoint's GrafNav GPS processing software calculated DGPS positions using raw range data obtained from receivers in the aircraft and at a fixed ground base station.

The GPS ground station position was determined by sending several hours of collected data to an online GPS processing service to obtain a differentially corrected computed position. The service selected was AUSPOS, which is provided by Geoscience Australia. The GPS data were processed, and quality controlled using the WGS84 datum.

Parameters for the WGS84 datum are:

Ellipsoid: WGS84

Semi-major axis: 6,378,137.0 m

Inverse flattening (1/f): 298.257

All processing was performed using WGS84/UTM Zone 18N coordinates. Final line data and final grid data were supplied in this projection.

5.5 Terrain Correction

Terrain corrections were derived from the digital terrain model grid for every data point in the survey. A terrain density of 1.00 g/cm^3 was used to compute the terrain correction channels, which were then multiplied by the chosen correction density before being subtracted from the data.

In the absence of any knowledge of the local geology, the standard correction density of 2.67 g/cm^3 was selected. Typically, 2.67 g/cm^3 will work well for most terrain types but may lead to over correction or under correction in some areas.

5.6 Tie line Levelling

The terrain corrected data and the uncorrected data were then tie line levelled separately for each block.

5.7 Enhanced Processing

The enhanced processing technique improves the noise amplitude density (as discussed by Christensen et al, 2015) by 25-50% for surveys with line spacing of less than 1 km. The method exploits the different spatial frequencies of system noise and geologic signal. After converting the data into the 2D spatial domain, a custom spatial filter is applied that removes the system

noise, while retaining the remaining geologic signal. The process will limit the data resolution to the survey line spacing.
FALCON® Airborne Gravity Gradient Data - G_{DD} & g_D

The transformation into G_{DD} and g_D was accomplished using a Fourier domain transformation method.

5.7.1 Fourier

The Fourier domain transformation method firstly calculates many flat surfaces at constant intervals between the lowest and highest-flying altitude. The transformation is performed on each of these surfaces and the result is a three-dimensional array for each tensor component where each level corresponds to a flat layer of a constant flying height. Using an approximation, the data is interpolated from this array back onto the processing drape surface.

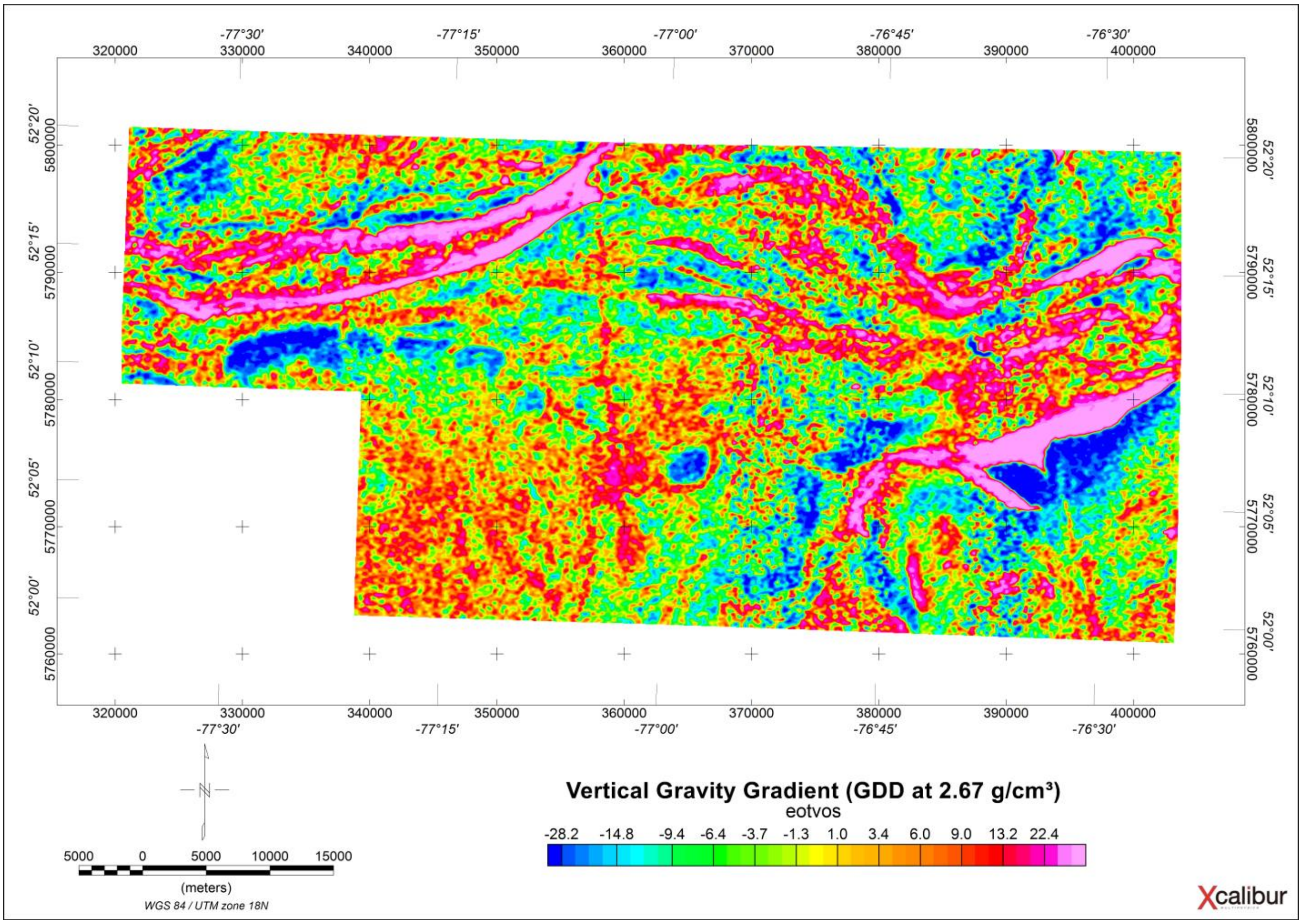

Figure 9: Baie-James bloc EST and OUEST – Enhanced Vertical Gravity Gradient (GDD) from Fourier processing (eotvos).

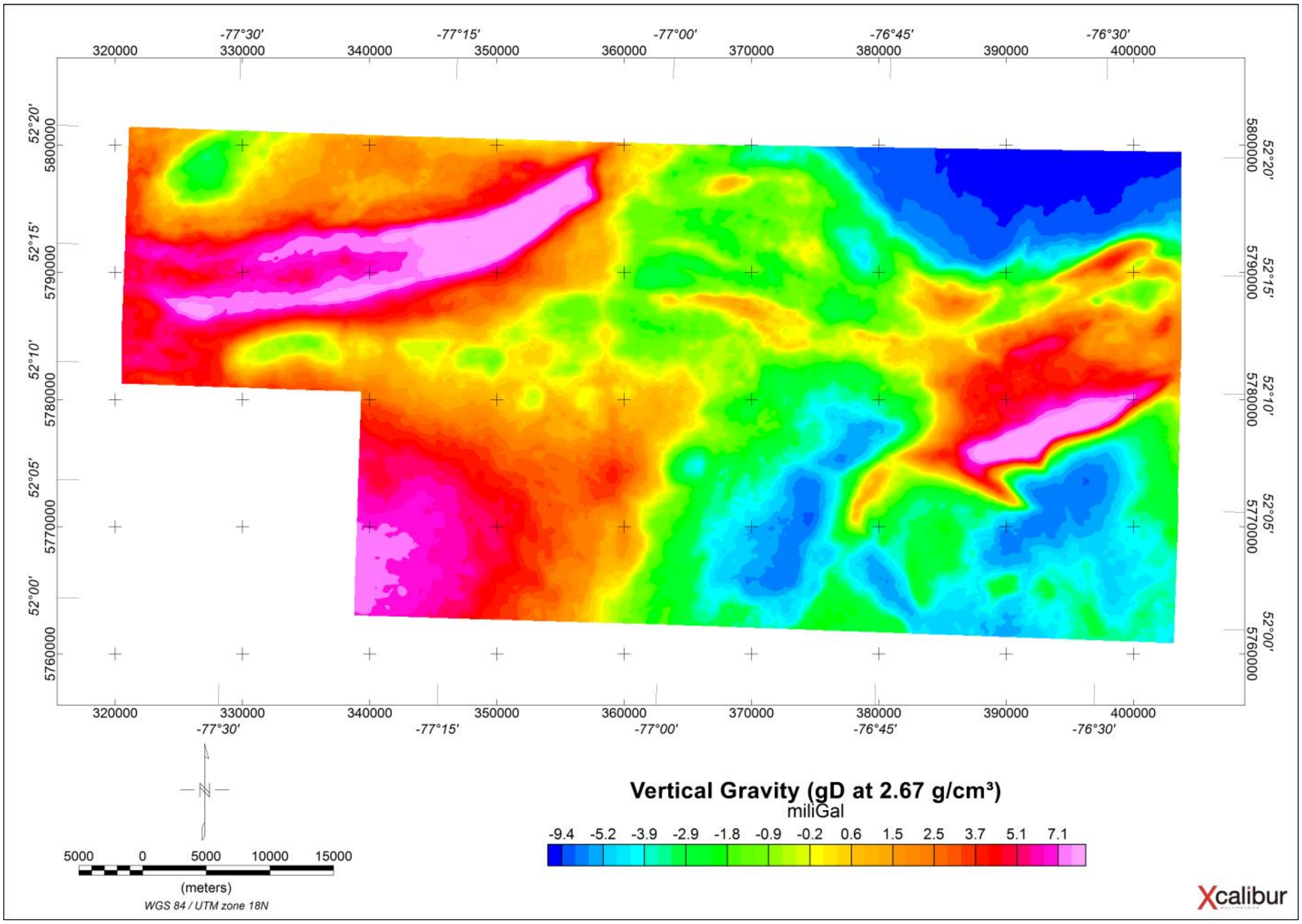

Figure 10: Baie-James bloc EST and OUEST – Enhanced Vertical Gravity (gD) from Fourier processing (milligal)

5.8 Conforming gD to regional gravity

As discussed in section *9.3,* the long wavelength information in g_D and G_{DD} can be improved by incorporating ancillary information. Such information is available in the form of the Canadian Gravity Anomaly Data Base.

The Fourier gD and GDD grids were conformed to grids derived from a subset of the Canadian Gravity Anomaly Data Base as follows.

- Low pass filter the regional data using a cosine squared filter with cut-off at 30 km, tapering to 20 km.
- High pass filter the g_D and G_{DD} data using a cosine squared filter with cut-off at 30 km, tapering to 20 km.
- Conform the g_D and G_{DD} data to the regional data by addition of the filtered grids. The filter design is such that this method provides uniform frequency response across the overlap frequencies.

The terrain corrected results using a density of 2.67 g/cm^3 are presented in *Figure 11* and *Figure 12*.

Further discussion of this method can be found in Dransfield (2010).

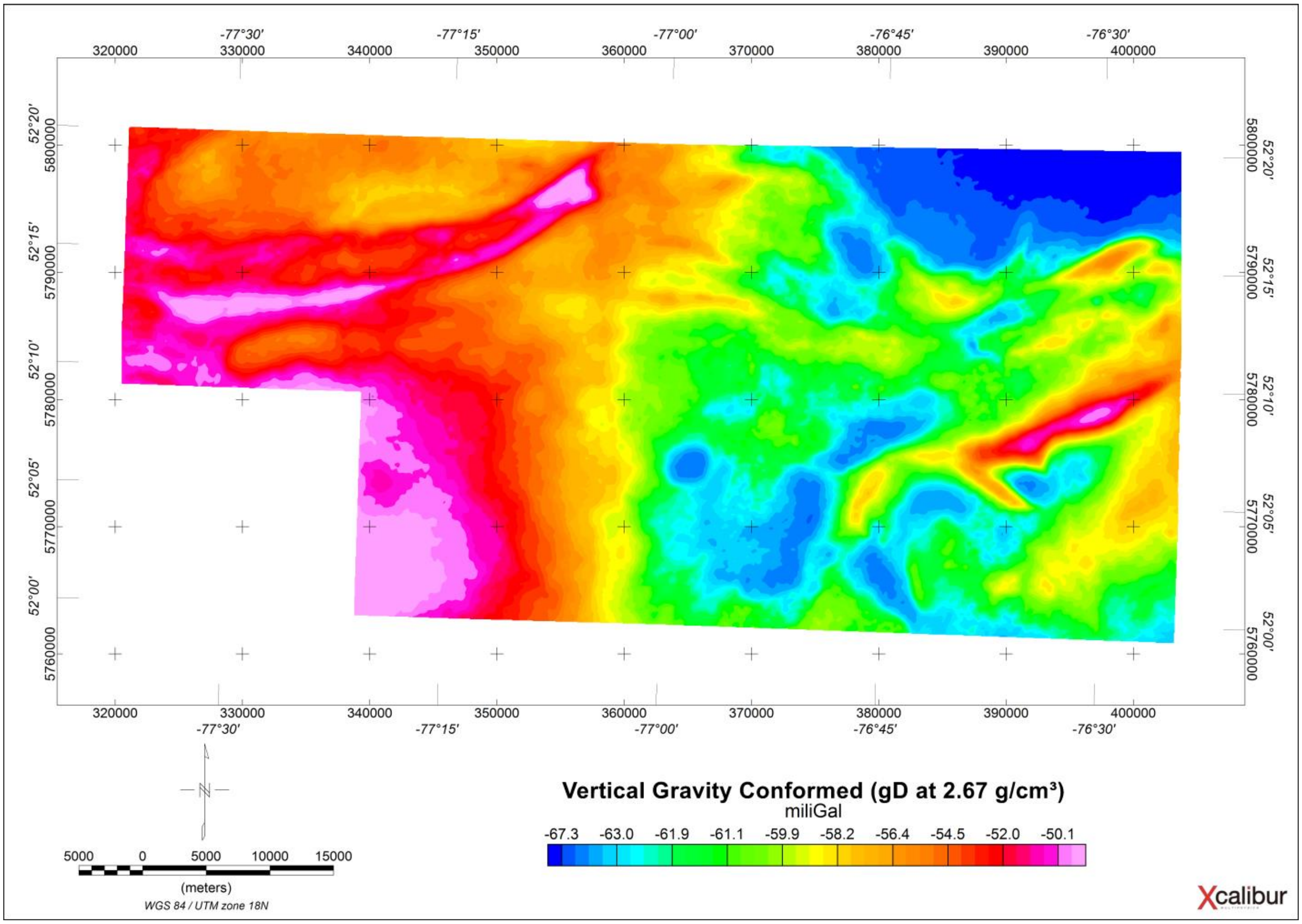

Figure 11: Baie-James bloc EST and OUEST – Enhanced Vertical Gravity (gD) from Fourier processing conformed to regional gravity data (milligal)

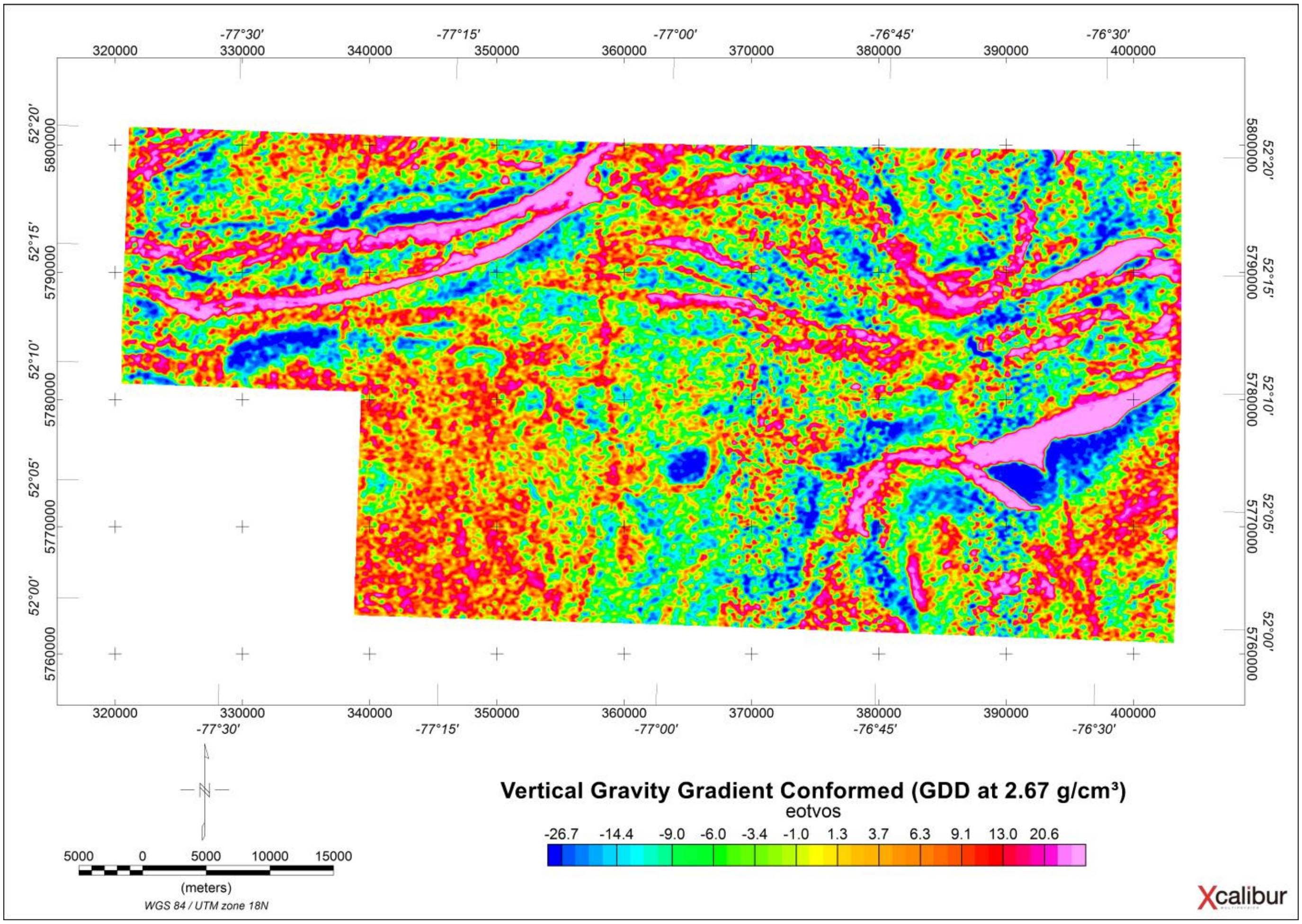

Figure 12: Baie-James bloc EST and OUEST – Enhanced Vertical Gravity Gradient (GDD) conformed to regional gravity data (eotvos).

6 AEROMAGNETIC RESULTS

6.1 Processing Summary

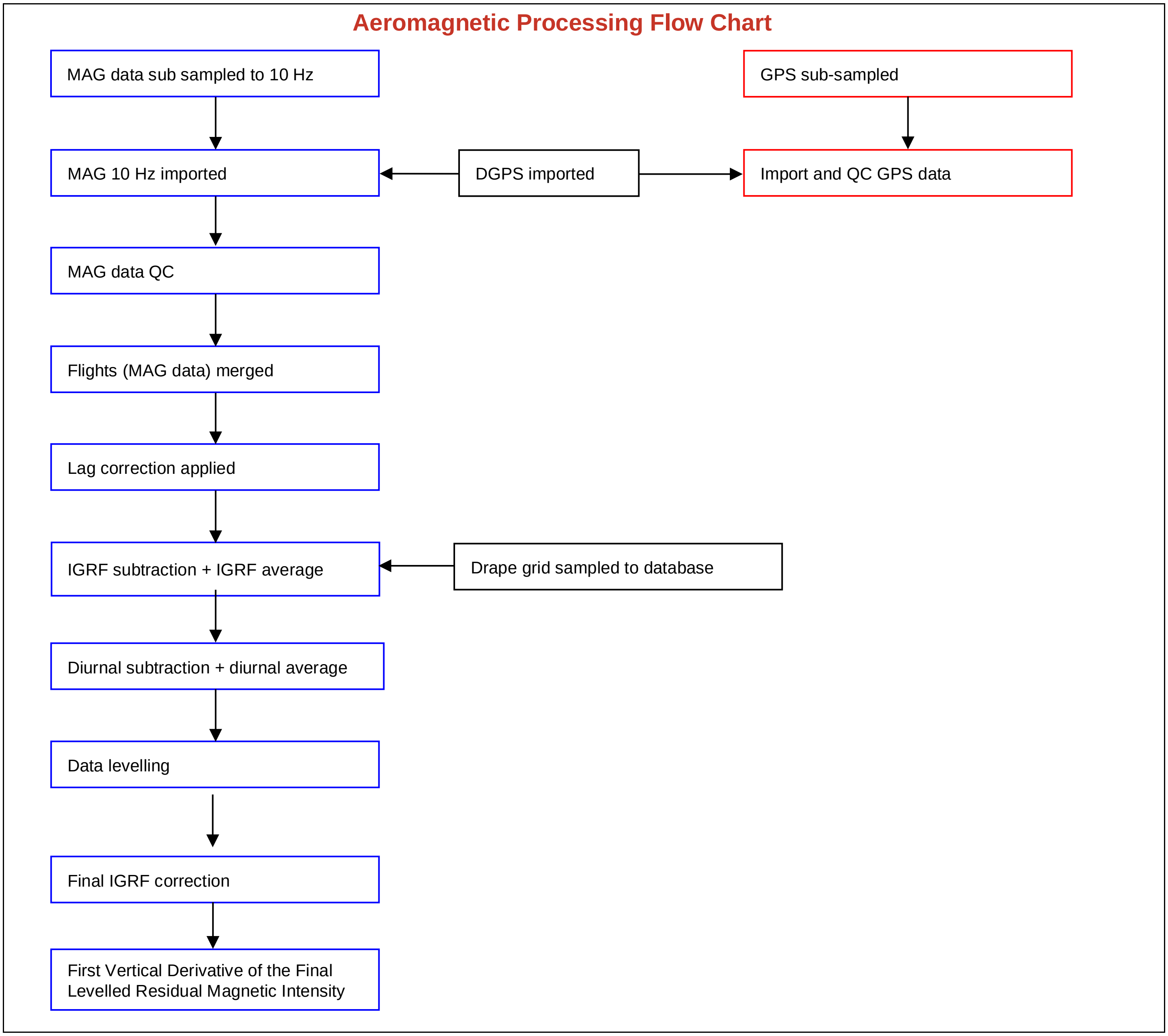

Figure 13: Aeromagnetic Data Processing

6.2 Aeromagnetic Data

Figure 13 summarises the steps involved in processing the aeromagnetic data obtained from the survey.

The aeromagnetic data were digitally recorded by the FASDAS on removable hard drives. The raw data were then copied onto the field processing laptop, backed up twice onto hard drive media and sent via FTP to Xcalibur Multiphysics' secure server.

Preliminary QC of the aeromagnetic data was completed on-site using Xcalibur Multiphysics' proprietary ATLAS software. Further QC and aeromagnetic data processing were performed by the office-based data processor.

6.3 Positional Data

Refer to section *5.4* for positional data processing.

6.4 Lag Correction

All aeromagnetic data were lagged prior to final processing. A lag of 0.4 seconds was applied.

6.5 IGRF Correction

The IGRF model 2020 was calculated at date 7^{th} Jan 2022, using the GPS height for each magnetic reading. This value was subtracted from each magnetic reading to produce an IGRF corrected residual magnetic intensity.

6.6 Diurnal Subtraction

The edited base station magnetics (diurnal) were filtered using a long wavelength filter to retain wavelengths longer than 51 seconds. This value was subtracted from the IGRF corrected total magnetic intensity. Next, based upon the average magnetic value calculated from running the base station for 24 hours, a base value of 56234.3 nT was added back to the magnetics. This produced the diurnally corrected total magnetic intensity.

6.7 Tie line Levelling

The IGRF and diurnally corrected total magnetic intensity data were tie line levelled using Xcalibur Multiphysics' proprietary ATLAS software.

6.8 Micro-levelling

The total magnetic intensity data were micro-levelled using Xcalibur Multiphysics' proprietary ATLAS software.

6.9 Final IGRF Correction

The levelled total magnetic intensity data were then IGRF corrected using the 2020 model, 2022/01/07 as the removal date and a constant elevation of 272.6 m above the WGS84 ellipsoid. The output from this correction is the residual magnetic intensity.

6.10 Final Magnetic Intensity

The final magnetic intensity is presented in *Figure 14*.

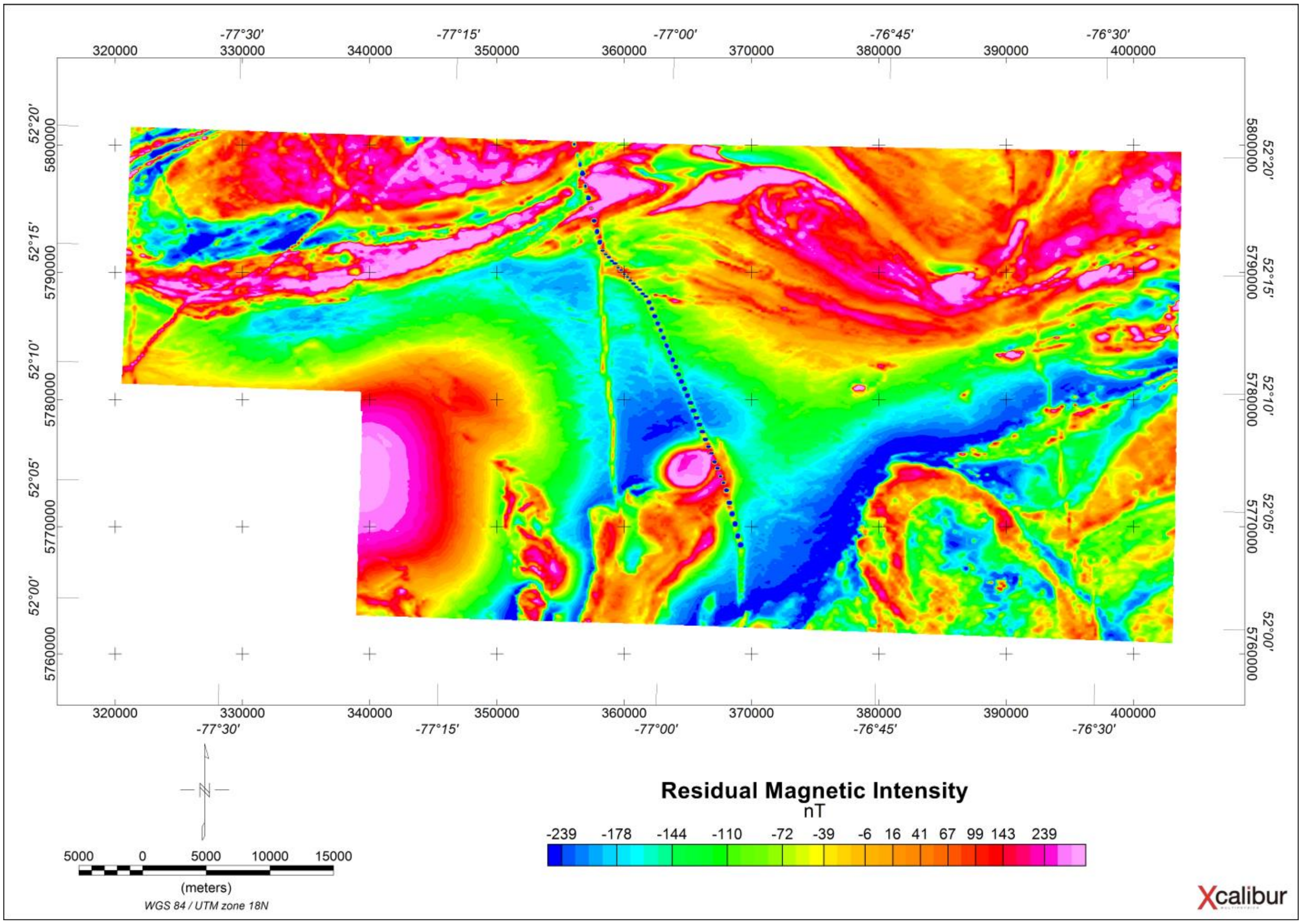

Figure 14: Baie-James bloc EST and OUEST – Final Magnetic Intensity (nT)

6.11 First Vertical Derivative of the Final Magnetic Intensity

The first vertical derivative of the final magnetic intensity is presented in *Figure 15*.

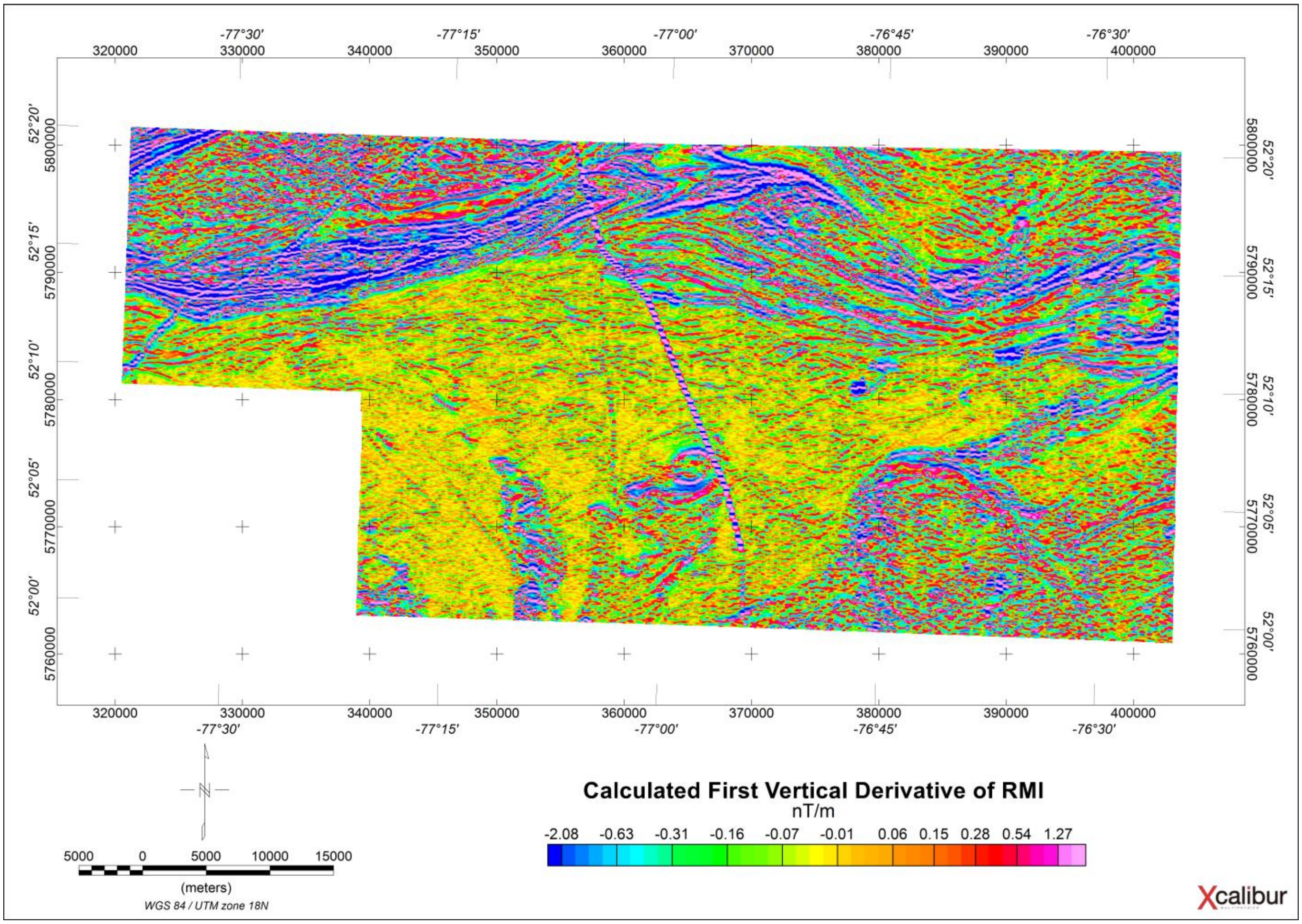

Figure 15: Baie-James bloc EST and OUEST – First Vertical Derivative of the Final Magnetic Intensity (nT/m)

7 APPENDIX I - SURVEY EQUIPMENT

7.1 Survey Aircraft

Xcalibur Multiphysics utilized three company aircraft to conduct the survey: A Cessna C208B turbo prop, Canadian registration C-GGRD equipped with a digital **FALCON®** AGG System (Kepler), a Cessna C208B turbo prop, Canadian registration C-FXAG equipped with a digital **FALCON®** AGG System (Kepler), and a Basler BT67 turbo prop, Canadian registration C-GGSU equipped with an analog **FALCON®** AGG System (Galileo).

7.2 FALCON® Airborne Gravity Gradiometer

FALCON® AGG System (Galileo and Kepler)

The **FALCON®** AGG Analog and Digital Systems are based on current state-of-the-art airborne gravity gradiometer technology and have been optimized for airborne broadband geophysical exploration. The systems are capable of supporting surveying activities in areas ranging from 1,000 ft below sea level to 13,000 ft above sea level with aircraft speeds from 30 to 130 knots.

The **FALCON®** AGG Analog System (Galileo) was installed on the Basler aircraft C-GGSU for the duration while the **FALCON®** AGG Digital System (Kepler) was initially installed on the Cessna aircraft C-GGRD for operations in 2021 and then moved to the Cessna aircraft C-FXAG for continued operations in 2022.

Noise specification for the Analog System (Galileo) is 5.0 eotvos or less in the gradient curvature components for any line while for the Digital System (Kepler) the noise specifications is 2.5 eotvos or less in the gradient curvature components for any line. Curvature gradient noise for each curvature component is calculated as the standard deviation, over each survey line, of half of the difference between the complements after filtering with the Demodulation Filter

The FALCON® AGG data streams were digitally recorded at different rates on removable drives installed in the FALCON® AGG electronics rack.

7.3 Airborne Data Acquisition Systems

Digital Acquisition System (FASDAS)

The FASDAS is a data acquisition system executing propriety software for the acquisition and recording of location, magnetic and ancillary data. Data are presented both numerically and graphically in real time on the VGA display providing on-line quality control capability.

The FASDAS is also used for real time navigation. A pre-programmed flight plan, containing boundary coordinates, line start and end coordinates, altitude values calculated for a theoretical drape surface, line spacing and cross track definitions is loaded into the computer prior to each flight. The WGS84 latitude, longitude and altitude received from the real-time corrected, dual frequency Novatel positioning receiver, is transformed to the local coordinate system for cross track and distance to go values. This information, together with ground heading and speed, is displayed to the pilot numerically and graphically on a two-line LCD display. It is also presented on the operator LCD screen in conjunction with a pictorial representation of the survey area, survey lines and ongoing flight path.

FALCON® AGG Data Acquisition System (ADAS)

The ADAS provides control and data display for the FALCON® AGG system. Data are displayed in real time for the operator and warnings displayed should system parameters deviate from tolerance specifications. All FALCON® AGG and laser scanner data are recorded to a removable hard drive.

7.4 Aerial and Ground Magnetometers

The airborne Caesium magnetometer was a **Scintrex CS-3** having a noise envelope of 0.05 nT pk-pk, 0.1 Hz bandwidth.

The ground magnetometer was a **Scintrex CS-3** Caesium sensor sampling at 1 Hz.

7.5 Real-Time Differential GPS

The **Novatel OEMV-3G** multi-frequency positioning receiver provides real-time differential GNSS for the on-board navigation system. The OEMV-3 is designed to track the GPS L1 and L2 signals, as well as GLONASS L1 and L2. The differential data set is relayed via a geo-synchronous satellite to the aircraft where the receiver optimized the corrections for the current location.

7.6 GPS Base Station Receiver

The **Novatel OEM4** is a multi-channel, L1/L2 GNSS receiver. It provides raw range information of all satellites in view sampled every second and recorded on a computer laptop. These data are used to provide post-processed differential GNSS (DGNSS) corrections for the rover data flight path.

7.7 Laser Scanner

Riegl LMS-Q240I-60

The laser scanner is designed for high-speed line scanning applications. The system is based upon the principle of time-of-flight measurement of short laser pulses in the infrared wavelength region and the angular deflection of the laser beam is obtained by a rotating polygon mirror wheel. The measurement range is up to 650 m with a minimum range of 2 m and an accuracy of 20 mm. The laser beam is eye-safe, the laser wavelength is 0.9 μm, the scan angle range is ± 40° and the scan speed is 36 scans/s.

Riegl VUX-1UAV

The laser scanner is designed for high-speed line scanning applications in conjunction with an external IMU unit. The system is based upon the principle of time-of-flight measurement of short laser pulses in the near infrared wavelength region and the angular deflection of the laser beam is obtained by a rotating polygon mirror wheel. At a laser pulse repetition rate of 51.48 kHz, the measurement range is up to 1050 m (depending on reflectivity) with a minimum range of 3 m and an accuracy of 10 mm (1 sigma @ 150 m range under Riegl test conditions). The laser beam is eye-safe, the laser wavelength is near infrared, the scan angle range is up to ± 80º and the scan speed is up to 200 scans/s.

7.8 Data Processing Hardware and Software

The following equipment and software were used:

Hardware

- One 2.0 GHz (or higher) laptop computer
- External USB hard drive reader for ADAS removable drives
- Two External USB hard drives for data backup
- All-In-One printer, copier, scanner

Software

- Oasis Montaj data processing and imaging software
- GrafNav Differential GPS processing software
- Xcalibur Multiphysics' Atlas data processing software
- Xcalibur Multiphysics' DiAGG processing software

8 APPENDIX II - SYSTEM TESTS

8.1 Instrumentation Lag

Due to the relative position of the magnetometer, altimeters and GPS antenna on the aircraft and to processing/recording time lags, raw readings from each data stream vary in position. To correct for this and to align selected anomaly features on lines flown in opposite directions, the magnetic and altimeter data are 'parallaxed' with respect to the position information. The lags were applied to the data during processing.

8.2 Radar Altimeter Calibration

The radar altimeter is checked for accuracy and linearity every 12 months, or when any change in a key system component requires this procedure to be carried out. This calibration allows the radar altimeter data to be compared and assessed with the other height data (GPS, barometric and laser) to confirm the accuracy of the radar altimeter over its operating range. The calibration is performed by flying a number of 30-second lines at preselected terrain clearances over an area of flat terrain and using the results of the radar altimeter, differentially corrected GPS heights in mean sea level (MSL) and laser scanner were used to derive slope and offset information.

8.3 Magnetometer Compensation

The magnetometer compensation corrects the magnetometer readings for the effect of the magnetic field of the aircraft, both static and dynamic, on the readings.

The compensation correction is calculated using a fluxgate magnetometer to measure the aircraft's manoeuvres. Manoeuvres consist of +/-5 degree rolls, +/-10 degree pitches and +/-5 degree yaws peak to peak over periods of 5 seconds repeated in each line direction. The magnetometer compensation is repeated when a change big enough to impact on the magnetometer has been made to the aircraft or its contents. A magnetometer compensation is normally performed in an area with similar magnetic declination, inclination and field strength to the survey area, i.e. close to or within the survey area.

8.4 FALCON® AGG Noise Measurement

At the commencement of the survey, 20 minutes of data were collected with the aircraft in straight level flight at 3500 ft AGL. These data were assessed in-flight to check the AGG noise levels.

Daily flight debriefs incorporating **FALCON®** AGG performance statistics for each flight line are prepared using output from Xcalibur Multiphysics' DiAGG software. These are sent daily to Xcalibur Multiphysics' office staff for performance evaluation.

8.5 Daily Calibrations

A set of daily calibrations were performed each survey day as follows:

- Magnetic base station time check
- AGG Quiescent Calibration

8.5.1 Magnetic Base Station Time Check

Prior to each day's survey, all magnetic base stations were synchronised using broadcast GPS time signals.

8.5.2 FALCON® AGG Calibration

A calibration was performed at the beginning of each flight and the results monitored by the operator. The coefficients obtained from each of the calibrations were used in the processing of the data.

9 APPENDIX III - FALCON® AGG DATA & PROCESSING

9.1 Nomenclature

The **FALCON®** airborne gravity gradiometer (AGG) system adopts a North, East, and Down coordinate sign convention and these directions (N, E, and D) are used as subscripts to identify the gravity gradient tensor components (gravity vector derivatives). Lower case is used to identify the components of the gravity field and upper case to identify the gravity gradient tensor components. Thus, the parameter usually measured in a normal exploration ground gravity survey is $\mathbf{g_D}$ and the vertical gradient of this component is $\mathbf{G_{DD}}$.

9.2 Units

The vertical component of gravity ($\mathbf{g_D}$) is delivered in the usual units of mGal. The gradient tensor components are delivered in eotvos, which is usually abbreviated to "E". By definition **1 E = 10^{-4} mGal/m.**

9.3 FALCON® Airborne Gravity Gradiometer Surveys

In standard ground gravity surveys, the component measured is "$\mathbf{g_D}$", which is the *vertical component of the acceleration due to gravity*. In airborne gravity systems, since the aircraft is itself accelerating, measurement of "$\mathbf{g_D}$" cannot be made to the same precision and accuracy as on the ground. Airborne gravity gradiometry uses a differential measurement to remove the aircraft motion effects and delivers gravity data of a spatial resolution and sensitivity comparable with ground gravity data.

The **FALCON®** gradiometer instrument acquires two curvature components of the gravity gradient tensor namely $\mathbf{G_{NE}}$ and $\mathbf{G_{UV}}$ where $\mathbf{G_{UV}} = (\mathbf{G_{NN}} – \mathbf{G_{EE}})/2$.

A feature of the **FALCON®** AGG system is that two independent measurements are made of both the NE and UV curvature components. This is achieved by using two sets of accelerometers, referred to as the A complement and the B complement. Each complement consists of four accelerometers. The measured gradients from these complements are referred to as A_{NE} and A_{UV} and B_{NE} and B_{UV}. The $\mathbf{G_{NE}}$ and $\mathbf{G_{UV}}$ gradients are computed by averaging A and B:

$$\boldsymbol{G_{NE}} = \frac{(A_{NE} + B_{NE})}{2}$$

$$\boldsymbol{G_{UV}} = \frac{(A_{UV} + B_{UV})}{2}$$

Since these curvature components cannot easily and intuitively be related to the causative geology, they are transformed into the vertical gravity gradient ($\mathbf{G_{DD}}$), and integrated to derive the vertical component of gravity ($\mathbf{g_D}$). Interpreters display, interpret and model both $\mathbf{G_{DD}}$ and $\mathbf{g_D}$. The directly measured $\mathbf{G_{NE}}$ and $\mathbf{G_{UV}}$ data are appropriate for use in inversion software to generate density models of the earth. The vertical gravity gradient, $\mathbf{G_{DD}}$, is more sensitive to small or shallow sources and has greater spatial resolution than $\mathbf{g_D}$ (similar to the way that the vertical magnetic gradient provides greater spatial resolution and increased sensitivity to shallow sources of the magnetic field). In the integration of $\mathbf{G_{DD}}$ to give $\mathbf{g_D}$, the very long wavelength component, at wavelengths comparable to or greater than the size of the survey area, cannot be fully recovered. Long wavelength gravity data are therefore incorporated in the $\mathbf{g_D}$ data from other sources. This might be regional ground, airborne or marine gravity if such data are available. The Danish Technical University global gravity data of 2013 (DTU13) are used as a default if other data are not available.

9.4 Gravity Data Processing

The main elements and sequence of processing of the gravity data are given below. Unless not applicable or specified otherwise, the processing step is applied to each individual complement element (A_{NE}, A_{UV}, B_{NE}, B_{UV}):

1. Dynamic corrections for residual aircraft motion (called Post Mission Compensation or PMC) are calculated and applied.

2. Self-gradient corrections are calculated and applied to reduce the time-varying gradient response from the aircraft and platform.
3. A Digital Terrain Model (DTM) is created from the laser scanner range data, the AGG inertial navigation system rotation data and the DGPS position data.
4. Terrain corrections are calculated and applied.
5. Line levelling and micro-levelling (where necessary) are applied.
6. $\mathbf{G_{NE}}$ and $\mathbf{G_{UV}}$ are transformed into the full gravity gradient tensor, including $\mathbf{G_{DD}}$, and into $\mathbf{g_D}$.

9.5 Aircraft Dynamic Corrections

The design and operation of the **FALCON®** AGG results in very considerable reduction of the effects of aircraft acceleration but residual levels are still significant and further reduction is required and must be done in post-processing.

Post-processing correction relies on monitoring the inertial acceleration environment of the gravity gradiometer instrument (GGI) and constructing a model of the response of the GGI to this environment. Parameters of the model are adjusted by regression to match the sensitivity of the GGI during data acquisition. The modelled GGI output in response to the inertial sensitivities is subtracted from the observed output. Application of this technique to the output of the GGI, when it is adequately compensated by its internal mechanisms, reduces the effect of aircraft motion to acceptable levels.

Following these corrections, the gradient data are demodulated and filtered along line using a 6-pole Butterworth low-pass filter with a cut-off frequency of 0.18 Hz.

9.6 Self-gradient Corrections

The GGI is mounted in gimbals controlled by an inertial navigation system, which keeps the GGI pointing in a fixed direction whilst the aircraft and gimbals rotate around it. Consequently, the GGI measures a time-varying gravity gradient due to these masses moving around it as the heading and attitude of the aircraft changes during flight. This is called the self-gradient.

Like the aircraft dynamic corrections, the self-gradient is calculated by regression of model parameters against measured data. In this case, the rotations of the gimbals are the input variables of the model. Once calculated, the modelled output is subtracted from the observed output.

9.7 Laser Scanner Processing

The laser scanner measures the range from the aircraft to the ground in a swath of angular width ±40/80 degrees below the aircraft. The aircraft attitude (roll, pitch and heading) data provided by the AGG inertial navigation system are used to adjust the range data for changes in attitude and the processed differential GPS data are used to reference the range data to located ground elevations referenced to the WGS84 datum (corrected for the EGM96 geoid separation model). Statistical filtering strategies are used to remove anomalous elevations due to foliage or built-up environment. The resulting elevations are gridded to form a digital terrain model (DTM).

9.8 Terrain Corrections

An observation point above a hill has excess mass beneath it compared to an observation point above a valley. Since gravity is directly proportional to the product of the masses, uncorrected gravity data have a high correlation with topography.

It is therefore necessary to apply a terrain correction to gravity survey data. For airborne gravity gradiometry at low survey heights, a detailed DTM is required. Typically, immediately below the aircraft, the digital terrain will need to be sampled at a cell size roughly one-third to one-half of the survey height and with a position accuracy of better than 1 metre. For these accuracies, LIDAR data are required and each **FALCON®** survey aircraft comes equipped with LIDAR (laser scanner).

If bathymetric data are used, then these form a separate terrain model for which terrain corrections are calculated at a density chosen to suit the water bottom – water interface.

Once the DTM has been merged, the terrain corrections for each of the $\mathbf{G_{NE}}$ and $\mathbf{G_{UV}}$ data streams are calculated. In the calculation of terrain corrections, a density of 1 g/cm^3 is used. The calculated corrections are stored in the database allowing the use of any desired terrain correction density by subtracting the product of desired density and correction from the measured $\mathbf{G_{NE}}$ and $\mathbf{G_{UV}}$ data. The terrain correction density is chosen to be representative of the terrain density over the survey area. Sometimes more than one density is used with input from the Client.

Typically, the terrain corrections are calculated over a distance 40 to 60 km from each survey measurement point.

9.9 Tie line Levelling

The terrain and self-gradient corrected $\mathbf{G_{NE}}$ and $\mathbf{G_{UV}}$ data are tie line levelled across the entire survey using a least-squares minimisation of differences at survey line intersections. Occasionally some micro-levelling might be performed.

9.10 Regional Levelling

The terrain and self-gradient corrected $\mathbf{G_{NE}}$ and $\mathbf{G_{UV}}$ data are adjusted to the regional data, separately for each line. Occasionally some micro-levelling might be performed.

9.11 Transformation into GDD & g_D

The transformation of the measured, corrected and levelled $\mathbf{G_{NE}}$ and $\mathbf{G_{UV}}$ data into gravity and components of the full gravity gradient tensor is accomplished using two methods:

- Fourier domain transformation

The input data for the Fourier method are the average **NE** and **UV** components computed from the complement data, as described in section *9.3*. The Fourier method relies on the Fourier transform of Laplace's equation. The application of this transform to the complex function $\mathbf{G_{NE} + i\, G_{UV}}$ provides a stable and accurate calculation of each of the full tensor components and gravity. The Fourier method performs piece-wise upward and downward continuation to work with data collected on a surface that varies from a flat horizontal plane. For stability of the downward continuation, the data are low-pass filtered. The cut-off wavelength of this filter depends on the variations in altitude range and line spacing. It is set to the smallest value that provides stable downward continuation.

In survey areas where the variability of the terrain surface (and hence the flight surface) makes it impossible to obtain Fourier transformation results that are both high resolution and stable, an alternate method can be applied which bypasses the upward and downward continuation steps. The results are calculated at the flight surface. This approach lacks the mathematical rigour of the complete method but allows for greater detail in the output data. It must be noted however that, if the terrain is too extreme, this method may fail to accurately transform the input data. This can be checked by comparing the input GNE and GUV data with the predicted values of the same data after transformation. If they do not match well, the Fourier transformation method cannot be relied upon.

The limitations of gravity gradiometry in reconstructing the long wavelengths of gravity can lead to differences in the results of these two methods at long wavelength. The merging of the $\mathbf{g_D}$ data with externally supplied regional gravity such as the DTU13 gravity provides a way of reducing these differences. The application of this procedure will depend on the survey size and resolution of available regional gravity. If survey size is too small or regional gravity resolution too large, regional conforming is not applied.

9.12 Terrain Corrections Using Alternate Terrain Densities

Although both uncorrected processed and transformed data and unit density terrain correction data are supplied, it is not recommended that these be used to create final data corrected for any arbitrary terrain correction density. The principal reason for this is that tie line levelling occurs after application of the terrain correction. As a result, levelling errors present in the terrain correction channels by virtue of positional inaccuracy are not removed from these channels and will be present in any data corrected with them. Further, filtering applied in creating the uncorrected, transformed data is not applied to the terrain correction channels. Mixing data filtered in different ways is not advised.

An alternative method (valid only for datasets where waterbody(ies) have not been taken into account when computing the terrain corrections) uses the linear relationship between the terrain corrections at different densities and the corresponding gravity gradient or $\mathbf{g_D}$ values. This method can be applied to either the grid data or the located data. An example is given using $\mathbf{G_{DD}}$:

The new density is referred to as ρ_N, the existing densities as ρ_1 and ρ_2

$$G_{DD}(\rho_N) = G_{DD}(\rho_1) + \left(G_{DD}(\rho_2) - G_{DD}(\rho_1)\right) \times \frac{(\rho_N - \rho_1)}{(\rho_2 - \rho_1)}$$

Note that the terrain correction channel is eliminated by substitution in deriving this equation.

It is recommended that two densities that differ by a reasonable value be used for this method, in order to minimise uncertainties caused by noise in the data. The values of 0.00 and 2.67 g/cm^3 usually delivered should be sufficient to yield useful results.

When the effect of waterbodies are included in deriving the terrain corrections (bathymetry data have been supplied, enabling the creation of a combined bathymetry and elevation grid to be used for the terrain correction); an alternative method is required. This method requires waterbody corrected gradients, or $\mathbf{g_D}$, as part of the equation, rather than the ρ_1 data.

The new density is referred to as ρ_N, the existing density is ρ_2 and *WB* refers to the supplied waterbody corrected data.

$$G_{DD}(\rho_N) = G_{DD_{WB}} + \left(G_{DD}(\rho_2) - G_{DD_{WB}}\right) \times \frac{(\rho_N)}{(\rho_2)}$$

9.13 Noise & Signal

By taking two independent measurements of the NE and UV curvature components at each sample point, it is possible to obtain a direct indication of the reliability of these measurements. The standard deviation of half the difference of the pairs of measurements - (A_{NE},B_{NE}) and (A_{UV},B_{UV}) - provides a good estimate of the survey noise:

$$Noise_{NE} = StdDev\left(\frac{(A_{NE} - B_{NE})}{2}\right)$$

$$Noise_{UV} = StdDev\left(\frac{(A_{UV} - B_{UV})}{2}\right)$$

These difference channels are calculated for each data point. The standard deviation across all data points is the figure quoted for the survey as a whole.

This difference error has been demonstrated to follow a 'normal' or Gaussian statistical distribution, with a mean of zero. Therefore, the bulk of the population (95%) will lie between -2σ and +2σ of the mean. For a typical survey noise estimate of, say, 3 E, 95% of the noise will be between -6 E and +6 E.

These typical errors in the curvature gradients translate to errors in $\mathbf{G_{DD}}$ of about 5 E and in $\mathbf{g_D}$ (in the shorter wavelengths) in the order of 0.1 mGal.

9.14 Risk Criteria in Interpretation

The risks associated with a **FALCON®** AGG survey are mainly controlled by the following factors.

- **Survey edge anomalies** – the transformation from measured curvature gradients to vertical gradient and vertical gravity gradient is subject to edge effects. Hence, any anomalies located within about 2 x line spacing of the edge of the survey boundaries should be treated with caution.
- **Single line anomalies** – for a wide-spaced survey, an anomaly may be present on only one line. Although it might be a genuine anomaly, the interpreter should note that no two-dimensional control can be applied.

- **Low amplitude (less than 2σ) anomalies** – Are within the noise envelope and need to be treated with caution if they are single line anomalies and close in diameter to the cut-off wavelengths used.
- **Residual topographic error anomalies** – Inaccurate topographic correction either due to inaccurate DTM or local terrain density variations may produce anomalies. Comparing the DTM with the G_{DD} map terrain-corrected for different densities is a reliable way to confirm the legitimacy of an anomaly.
- **The low density of water and lake sediments** – (if present) can create significant gravity and gravity gradient lows, which may be unrelated to bedrock geology. It is recommended that all anomalies located within lakes or under water be treated with caution and assessed with bathymetry if available.

9.15 References

Boggs, D. B. and Dransfield, M. H., 2004, Analysis of errors in gravity derived from the Falcon® airborne gravity gradiometer, Lane, R. (ed.), Airborne Gravity 2004 - Abstracts from the ASEG-PESA Airborne Gravity 2004 Workshop, Geoscience Australia Record 2004/18, 135-141.

Christensen A.N., Dransfield, M. H. and Van Galder C, 2015, Noise and repeatability of airborne gravity gradiometry, First Break, Volume 33, April 2015, 55 - 63.

Dransfield, M. H., 2010, Conforming Falcon gravity and the global gravity anomaly, Geophysical Prospecting, 58, 469-483.

Dransfield, M. H. and Lee, J. B., 2004, The FALCON® airborne gravity gradiometer survey systems, Lane, R. (ed.), Airborne Gravity 2004 - Abstracts from the ASEG-PESA Airborne Gravity 2004 Workshop, Geoscience Australia Record 2004/18, 15-19.

Dransfield, M. H. and Zeng, Y., Airborne gravity gradiometry: terrain corrections and elevation error, Geophysics 2009/Sep 74(5).

Lee, J. B., 2001, FALCON Gravity Gradiometer Technology, Exploration Geophysics, 32, 75-79.

Lee, J. B.; Liu, G.; Rose, M.; Dransfield, M.; Mahanta, A.; Christensen, A. and Stone, P., 2001, High resolution gravity surveys from a fixed wing aircraft, Geoscience and Remote Sensing Symposium, 2001. IGARSS '01. IEEE 2001 International, 3, 1327-1331.

Stone, P. M. and Simsky, A., 2001, Constructing high resolution DEMs from Airborne Laser Scanner Data, Preview, Extended Abstracts: ASEG 15th Geophysical Conference and Exhibition, August 2001, Brisbane, 93, 99.

10 APPENDIX IV – CERTIFICATE OF REVIEWER

I, Mihai Szentesy, do hereby certify that:

1. I am residing at 511- 2100 Rue Du Coliseé, Longueuil, J4N 0C7, Québec, Canada.

2. I am temporary employed as Senior Geophysical Data Processor for the Toronto office of the geophysical survey firm Xcalibur Multiphysics.

3. I hold the following academic qualifications: B.Sc., Geology and Geophysics (1982), University of Babes-Bolyai, Cluj-Napoca, Romania.

4. I am a member in good standing of the Ordre des géologues du Québec (OGQ) since January 15th, 2013, member number #01747 and registered as a member of the Canadian Exploration Geophysical Society.

5. I have worked as a geologist for 10 years and in geophysical data processing for 11 years.

6. I have had no prior involvement with the Property that forms the subject of this Report.

7. I am not aware of any material fact or material change with respect to the subject matter of the Report that is not reflected in the Report, the omission to disclose which makes the Report misleading.

I have reviewed the Report titled "MINISTÈRE DE L'ÉNERGIE ET DES RESSOURCES NATURELLES FALCON® AIRBORNE GRAVITY GRADIOMETER AND MAGNETOMETER SURVEY, BAIE-JAMES, BLOC EST & OUEST, QUÉBEC, CANADA - Project Number: 2100365AB (117840512-20210207-06)" dated March 28th, 2022 and prepared for LE MINISTÈRE DE L'ÉNERGIE ET DES RESSOURCES NATURELLES.

Dated this 21st Day of September 2022.

Respectfully Submitted

Mihai Szentesy, Géologue Restrictif (1G3, #01747)

11 APPENDIX V - FINAL PRODUCTS

Final **FALCON**® AGG digital line data were provided in 8 Hz Geosoft Oasis GDB database files containing the fields and format described in *Table 4* below.

Final aeromagnetic digital line data were provided in 10 Hz Geosoft Oasis GDB database files containing the fields and format described in

Table 5 below.

Grids of Fourier AGG products, final magnetic intensity, first vertical derivative of the final magnetic intensity, as well as the DTM were delivered, as described in *Table 6* below. The grids are in GRD format with a 50 m cell size, with the exception of the DTM grid which has a 25 m cell size.

One copy of the digital archives was delivered along with a copy of this Logistics and Processing Report.

Variable	Units	Description
ALTITUDE	metres	GPS antenna height above sea level (referenced to EGM96 geoid)
ALTITUDE_DTM	metres	Flying height (aircraft's height above terrain)
ANE_0p0	eotvos	Self gradient corrected NE gradient with no terrain correction applied
ANE_2p67	eotvos	Self gradient & terrain corrected NE gradient using terrain correction density 2.67 g/cc
AUV_0p0	eotvos	Self gradient corrected UV gradient with no terrain correction applied
AUV_2p67	eotvos	Self gradient & terrain corrected UV gradient using terrain correction density 2.67 g/cc
BNE_0p0	eotvos	Self gradient corrected NE gradient with no terrain correction applied
BNE_2p67	eotvos	Self gradient & terrain corrected NE gradient using terrain correction density 2.67 g/cc
BUV_0p0	eotvos	Self gradient corrected UV gradient with no terrain correction applied
BUV_2p67	eotvos	Self gradient & terrain corrected UV gradient using terrain correction density 2.67 g/cc
DATE	YYYYMMDD	Gregorian date
DRAPESURFACE	metres	Drape surface for Fourier computation (smoothed flight surface)
DTM	metres	Terrain height above sea level (referenced to EGM96 geoid)
EASTING	metres	WGS84/UTM18N Easting
ERR_NE	eotvos	NE gradient uncorrelated noise estimate after levelling
ERR_UV	eotvos	UV gradient uncorrelated noise estimate after levelling
FLIGHT		Flight Number
gD_0p0	mGal	Fourier derived vertical gravity with no terrain correction applied
gD_0p0_conformed	mGal	Fourier derived vertical gravity with no terrain correction applied and conformed to regional gravity
gD_2p67	mGal	Fourier derived vertical gravity using terrain correction density 2.67 g/cc
gD_2p67_conformed	mGal	Fourier derived vertical gravity using terrain correction density 2.67 g/cc and conformed to regional gravity

GDD_0p0	eotvos	Fourier derived vertical gravity gradient with no terrain correction applied
GDD_0p0_conformed	eotvos	Fourier derived vertical gravity gradient with no terrain correction applied and conformed to regional gravity
GDD_2p67	eotvos	Fourier derived vertical gravity gradient using terrain correction density 2.67 g/cc
GDD_2p67_conformed	eotvos	Fourier derived vertical gravity gradient using terrain correction density 2.67 g/cc and conformed to regional gravity
GED_0p0	eotvos	Fourier derived Ged horizontal EW gradient with no terrain correction applied
GED_2p67	eotvos	Fourier derived Ged horizontal EW gradient using terrain correction density 2.67 g/cc
GEE_0p0	eotvos	Fourier derived Gee gradient with no terrain correction applied
GEE_2p67	eotvos	Fourier derived Gee gradient using terrain correction density 2.67 g/cc
GND_0p0	eotvos	Fourier derived Gnd horizontal NS gradient with no terrain correction applied
GND_2p67	eotvos	Fourier derived Gnd horizontal NS gradient using terrain correction density 2.67 g/cc
GNE_0p0	eotvos	Fourier derived Gne curvature gradient with no terrain correction applied
GNE_2p67	eotvos	Fourier derived Gne curvature gradient using terrain correction density 2.67 g/cc
GNN_0p0	eotvos	Fourier derived Gnn gradient with no terrain correction applied
GNN_2p67	eotvos	Fourier derived Gnn gradient using terrain correction density 2.67 g/cc
GUV_0p0	eotvos	Fourier derived Guv curvature gradient with no terrain correction applied
GUV_2p67	eotvos	Fourier derived Guv curvature gradient using terrain correction density 2.67 g/cc
LATITUDE	degrees	WGS84 latitude
LINE		Line Number
LONGITUDE	degrees	WGS84 longitude
NORTHING	metres	WGS84/UTM18N Northing
T_DD	eotvos	Terrain effect calculated for DD using a density of 1 g/cc (from final DTM grid)
T_NE	eotvos	Terrain effect calculated for NE using a density of 1 g/cc (from final DTM grid)
T_UV	eotvos	Terrain effect calculated for UV using a density of 1 g/cc (from final DTM grid)
TURBULENCE	milli g	Estimated vertical platform turbulence (vertical acceleration)
UTC_TIME1980	seconds	Universal Time (seconds since January 6, 1980)

Table 4: Final FALCON® AGG Digital Data –Geosoft Database Format

Variable	Units	Description
ALTITUDE	metres	GPS antenna height above sea level (referenced to EGM96 geoid)
ALTITUDE_DTM	metres	Flying height (aircraft height above terrain)
COMPMAG	nanoteslas	Lagged despiked compensated Total Magnetic Intensity
DATE	YYYYMMDD	Gregorian date
DCMAG	nanoteslas	CompMag after subtraction of the IGRF and Diurnal
DIURNAL	nanoteslas	Despiked lightly filtered ground station mag
DTM	metres	Terrain height above sea level (referenced to EGM96 geoid)
EASTING	metres	WGS84/UTM18N Easting
FLIGHT		Flight Number
FLUX_X	nanoteslas	Fluxgate X component
FLUX_Y	nanoteslas	Fluxgate Y component
FLUX_Z	nanoteslas	Fluxgate Z component
IGRF	nanoteslas	IGRF TMI based on location and altitude of each point
LATITUDE	degrees	WGS84 Latitude
LEVMAG_1VD	nanoteslas/metre	First Vertical Derivative of leveled and micro-levelled DCMAG
LEVMAG	nanoteslas	Leveled and micro-levelled DCMAG
LINE		Line Number
LONGITUDE	degrees	WGS84 Longitude
NORTHING	metres	WGS84/UTM18N Northing
RAWMAG	nanoteslas	Lagged despiked raw Total Magnetic Intensity
UTC_TIME1980	seconds	Universal Time (seconds since January 6, 1980)

Table 5: Final Aeromagnetic Digital Data –Geosoft Database Format

File	Description	Units
MERN_LEVMAG_final	Residual Magnetic Intensity	nT
MERN_LEVMAG_1VD_final	RMI First Vertical Derivative	nT/m
MERN_DTM	Terrain (height above EGM96 geoid), 25 m grid cell, with DEM-S extension (Trimmed for easy display)	metres
MERN_DTM_full	Terrain (height above EGM96 geoid), 25 m grid cell, with DEM-S extension, for AGG processing	metres
MERN_drape_surface	Drape surface for Fourier reconstruction (smoothed flight surface) height above EGM96 geoid	metres
MERN_gD_0p0_final	Enhanced Fourier derived vertical gravity, no terrain correction applied	mGal
MERN_gD_0p0_conformed_final	Enhanced Fourier derived vertical gravity, no terrain correction applied, conformed to regional gravity	mGal
MERN_GDD_0p0_final	Enhanced Fourier derived vertical gravity gradient, no terrain correction applied	eotvos

MERN_GDD_0p0_conformed_final	Enhanced Fourier derived vertical gravity gradient, no terrain correction applied, conformed to regional gravity	eotvos
MERN_gD_2p67_final	Enhanced Fourier derived vertical gravity, terrain correction density 2.67 g/cm^3	mGal
MERN_gD_2p67_conformed_final	Enhanced Fourier derived vertical gravity, terrain correction density 2.67 g/cm^3, conformed to regional gravity	mGal
MERN_GDD_2p67_final	Enhanced Fourier derived vertical gravity gradient, terrain correction density 2.67 g/cm^3	eotvos
MERN_GDD_2p67_conformed_final	Enhanced Fourier derived vertical gravity gradient, terrain correction density 2.67 g/cm^3, conformed to regional gravity	eotvos
MERN_GED_0p0_final	Enhanced Fourier derived horizontal EW gravity gradient, no terrain correction applied	eotvos
MERN_GED_2p67_final	Enhanced Fourier derived horizontal EW gravity gradient, terrain correction density 2.67 g/cm^3	eotvos
MERN_GEE_0p0_final	Enhanced Fourier derived Gee gradient, no terrain correction applied	eotvos
MERN_GEE_2p67_final	Enhanced Fourier derived Gee gradient, terrain correction density 2.67 g/cm^3	eotvos
MERN_GND_0p0_final	Enhanced Fourier derived horizontal NS gravity gradient, no terrain correction applied	eotvos
MERN_GND_2p67_final	Enhanced Fourier derived horizontal NS gravity gradient, terrain correction density 2.67 g/cm^3	eotvos
MERN_GNE_0p0_final	Enhanced Fourier derived gravity curvature gradient, no terrain correction applied	eotvos
MERN_GNE_2p67_final	Enhanced Fourier derived gravity curvature gradient, terrain correction density 2.67 g/cm^3	eotvos
MERN_GNN_0p0_final	Enhanced Fourier derived Gnn gradient, no terrain correction applied	eotvos
MERN_GNN_2p67_final	Enhanced Fourier derived Gnn gradient, terrain correction density 2.67 g/cm^3	eotvos
MERN_GUV_0p0_final	Enhanced Fourier derived gravity curvature gradient, no terrain correction applied	eotvos
MERN_GUV_2p67_final	Enhanced Fourier derived gravity curvature gradient, terrain correction density 2.67 g/cm^3	eotvos

Table 6: Final Aeromagnetic and FALCON® AGG Grids –Geosoft Format

12 APPENDIX VI - PRODUCTION REPORT

Upon signing of contract on September 28th, 2021, preparations of the system and test flying in Ottawa commenced. Mobilization of crew and aircraft to Radisson, Quebec began mid-October 2021 with first production flight flown October 20th, 2021.

The western portion of the survey (block B) flown with aircraft C-GGRD was completed October 31st.

12 survey flights were flown to cover block A over the course of 12 days with 3 days down due to weather conditions. There were no technical issues flying block B

The start of surveying on the eastern portion of the survey (block A) was delayed due to AGG system issues and aircraft laser scanner issues. The first survey flight in block A was conducted on October 30th using C-GGRD upon completion of block B. Replacement of the laser scanner in C-GGSU was required with parts arriving in Radisson on November 5th. Further issues of the AGG Galileo system required replacement of a computer board before becoming operational. While C-GGSU was not operational lines in block B were flown by C-GGRD.

Weather and temperatures throughout November and December caused significant delays in flying block B and caused issues in keeping the AGG system as a stable temperature for operations in C-GGSU. Issues were faced on the pre-flight system checks due to the extreme cold weather.

The survey was shutdown mid-December due to hotel shutdown over the Christmas and New Year's period. The hotel reopened January 10th but was only ready for crew after January 17th due to food logistics issues. Operator and engineer arrived on site on January 17th with aircraft delayed due to weather, arriving January 20th. A fuel leak was noticed the morning of January 21st on C-GGSU and it was determined repairs would have to be made at Basler Aircraft facilities in Wisconsin. The aircraft was demobilized from site. As an alternative to C-GGSU aircraft C-FXAG was prepared and AGG system installed. C-FXAG was mobilized to Radisson on February 5th.

Surveying recommenced in block B on February 6th and was completed February 12th.

14 survey flights were flown to cover block A over the course of 116 days. Significant down time due to AGG and laser scanner issues on C-GGSU were encountered amounting to 36 days. Weather also was a significant factor with 39 days down reported due to rain, snow, and high wind conditions. Ten of these weather days overlapped with system issue days and were reported primarily as system issues and secondary as weather. A further 37 days delay were due to hotel shutdown and food supply issues over the Christmas break and into the New Year.

The production report results are illustrated in the Table 7 below.

Date	Aircraft	Flight Number	Accepted Km	Rejected Km	Survey/Calibration/Aborted Flight
20-Oct-21	C-GGRD	201	181.26	20.14	Survey
21-Oct-21	C-GGSU	101	75.66	0.00	Survey
21-Oct-21	C-GGRD	202	0.00	0.00	FOM
23-Oct-21	C-GGRD	203	397.69	0.00	Survey
24-Oct-21	C-GGRD	204	377.20	188.60	Survey
24-Oct-21	C-GGRD	205	564.06	121.04	Survey
26-Oct-21	C-GGRD	206	595.56	0.00	Survey
27-Oct-21	C-GGRD	207	678.96	0.00	Survey
27-Oct-21	C-GGRD	208	443.08	37.72	Survey
28-Oct-21	C-GGRD	209	678.96	0.00	Survey
28-Oct-21	C-GGRD	210	503.70	0.00	Survey
29-Oct-21	C-GGRD	211	678.96	0.00	Survey
30-Oct-21	C-GGRD	212	377.20	0.00	Survey
30-Oct-21	C-GGRD	213	538.32	0.00	Survey
31-Oct-21	C-GGRD	214	680.06	0.00	Survey
3-Nov-21	C-GGRD	215	453.74	75.66	Survey
11-Nov-21	C-GGSU	104	113.45	37.83	Survey
15-Nov-21	C-GGSU	105	680.94	0.00	Survey
16-Nov-21	C-GGSU	106	945.75	37.83	Survey
17-Nov-21	C-GGSU	107	226.98	75.66	Survey
19-Nov--21	C-GGSU	108	0.00	0.00	FOM
26-Nov-21	C-GGSU	109	870.09	0.00	Survey
27-Nov-21	C-GGSU	110	0.00	37.83	Survey
6-Feb-22	C-FXAG	301	605.28	0.00	Survey
7-Feb-22	C-FXAG	302	605.28	75.66	Survey + FOM
7-Feb-22	C-FXAG	303	37.83	113.49	Survey
8-Feb-22	C-FXAG	304	75.66	75.66	Survey
11-Feb-22	C-FXAG	305	567.45	37.83	Survey
12-Feb-22	C-FXAG	306	567.45	37.83	Survey

Table 7: Production Report

13 APPENDIX IV - SYSTEM TESTS

Figure of Merit

Project Number: 2100365
Date Acquired: 21.10.2021
Compiled By: Aswin Lincoln
Flight: 2
Box: 3 on 2

Aircraft Registration: GRD
General Location: La Grande Riviere Airpor
Sensor Installation: Stinger

Max Specification (nT):
2

	Fiducial Range (s)	Uncompensated Mag (nT)	Compensated Mag (nT)	Improv. Ratio
Pitch		0.646	0.075	9
Roll		0.335	0.056	6
Yaw		0.235	0.079	3
Total		1.215	0.209	6

	Fiducial Range (s)	Uncompensated Mag (nT)	Compensated Mag (nT)	Improv. Ratio
Pitch		0.221	0.088	2
Roll		0.189	0.054	4
Yaw		0.210	0.104	2
Total		0.620	0.246	3

	Fiducial Range (s)	Uncompensated Mag (nT)	Compensated Mag (nT)	Improv. Ratio
Pitch		0.716	0.144	5
Roll		0.172	0.097	2
Yaw		0.271	0.355	1
Total		1.159	0.596	2

	Fiducial Range (s)	Uncompensated Mag (nT)	Compensated Mag (nT)	Improv. Ratio
Pitch		0.263	0.120	2
Roll		0.539	0.110	5
Yaw		0.131	0.067	2
Total		0.934	0.296	3

Uncompensated Mag (nT)	Compensated mag (nT)	Improv. Ratio
3.928	**1.348**	3

Table 8 Figure of Merit - Aircraft GRD

Figure of Merit

Project Number: 2100365
Date Acquired: 19.11.2021
Compiled By: Aswin Lincoln
Flight: 8
Box:

Aircraft Registration: GSU
General Location: La Grande Riviere Airport
Sensor Installation: Stinger

Max Specification (nT):
2

	Fiducial Range (s)	Uncompensated Mag (nT)	Compensated Mag (nT)	Improv. Ratio
Pitch		1.434	0.159	9
Roll		0.412	0.132	3
Yaw		0.342	0.151	2
Total		2.187	0.442	5

	Fiducial Range (s)	Uncompensated Mag (nT)	Compensated Mag (nT)	Improv. Ratio
Pitch		0.978	0.146	7
Roll		0.573	0.139	4
Yaw		0.342	0.112	3
Total		1.893	0.397	5

	Fiducial Range (s)	Uncompensated Mag (nT)	Compensated Mag (nT)	Improv. Ratio
Pitch		0.616	0.257	2
Roll		0.320	0.179	2
Yaw		0.322	0.200	2
Total		1.259	0.636	2

	Fiducial Range (s)	Uncompensated Mag (nT)	Compensated Mag (nT)	Improv. Ratio
Pitch		0.981	0.283	3
Roll		0.474	0.109	4
Yaw		0.485	0.101	5
Total		1.940	0.493	4

Uncompensated Mag (nT)	Compensated mag (nT)	Improv. Ratio
7.279	**1.969**	4

Table 9 Figure of Merit - Aircraft GSU

Figure of Merit

Project Number: 2100365 - MERN
Date Acquired: 07.02.2022
Compiled By: Jemal Mohammed-Nour
Flight: 2
Box: 812 using 810 cof

Aircraft Registration: FXAG
General Location: Radisson Quebec
Sensor Installation: Stinger

Max Specification (nT):
2

	Fiducial Range (s)	Uncompensated Mag (nT)	Compensated Mag (nT)	Improv. Ratio
Pitch	2471-2505	0.403	0.174	2
Roll	2515-2542	0.598	0.104	6
Yaw	2558-2571	0.204	0.112	2
Total		1.205	0.391	3

	Fiducial Range (s)	Uncompensated Mag (nT)	Compensated Mag (nT)	Improv. Ratio
Pitch	2637-2675	0.200	0.177	1
Roll	2691-2719	0.433	0.100	4
Yaw	2738-2750	0.134	0.087	2
Total		0.767	0.364	2

	Fiducial Range (s)	Uncompensated Mag (nT)	Compensated Mag (nT)	Improv. Ratio
Pitch	2806-2838	0.202	0.198	1
Roll	2858-2891	0.382	0.124	3
Yaw	2905-2916	0.103	0.093	1
Total		0.687	0.414	2

	Fiducial Range (s)	Uncompensated Mag (nT)	Compensated Mag (nT)	Improv. Ratio
Pitch	3008-3040	0.320	0.322	1
Roll	3067-3100	0.319	0.131	2
Yaw	3112-3120	0.139	0.194	1
Total		0.779	0.647	1

Uncompensated Mag (nT)	Compensated mag (nT)	Improv. Ratio
3.438	**1.816**	2

Table 10 Figure of Merit - Aircraft FXAG